

arXiv:hep-ph/9907247v1 6 Jul 1999

Screening in Hot Non-Abelian Plasma

(PhD Thesis)

Péter Petreczky

June 25, 1999

Eötvös Loránd University

Budapest

Supervisor:

András Patkós

Contents

1	Introduction	4
2	Review of non-Abelian Screening	6
2.1	Chromoelectric Screening at Leading Order	6
2.1.1	Chromoelectric Screening in Linear Response Theory	6
2.1.2	Debye screening from classical kinetic theory	7
2.1.3	Polyakov Loop Correlator and the Debye Screening	8
2.2	Infrared divergencies Associated with Static non-Abelian Magnetic Fields . .	11
2.3	Dimensional reduction	12
2.4	The Non-Abelian Debye Screening beyond Leading Order	13
2.4.1	Non-Abelian Debye Screening in One-Loop Resummed Perturbation Theory and the Magnetic Mass	13
2.4.2	Non-Perturbative definitions of the Debye mass	15
2.5	Screened Perturbation Theory	16
3	Coupled Gap Equation for the Screening Masses in Hot SU(N) Gauge Theory	19
3.1	Gauge non-invariant resummation scheme	19
3.2	Gauge Invariant Approach	22
3.3	Contribution of non-Local Operators to the Gap Equation	23
3.4	What Have We Learnt from the Coupled Gap Equations ?	25
4	Screening Masses of Hot SU(2) Gauge Theory from Monte-Carlo Simu- lation of the Lattice 3d Adjoint Higgs Model	27
4.1	The 3d SU(2) Adjoint Higgs Model on Lattice	28
4.2	Determination of the Propagators and the Screening Masses on Lattice . . .	29
4.3	Numerical Results for the Propagators of the 3d SU(2) Higgs Model	31
4.4	Magnetic Mass in 3d SU(2) Pure Gauge Theory	34
4.5	Gauge Invariant Correlators and the Additive Constituent Gluon Model . . .	35
4.6	Gauge Dependence of the Screening Masses	37
5	Coupled Gap Equation for SU(2) Higgs Model	40
5.1	The Extended Gap Equations	41
5.2	Numerical Results	44
5.3	Screening Masses in the Symmetric Phase with a Gauge Invariant Resumma- tion Scheme	48
6	Conclusions	51
A	Calculation of Different Diagrams in SU(N) Adjoint Higgs Model	53

B	3d Adjoint Higgs Model on Lattice	57
B.1	Phase Diagram of 3d Adjoint Higgs Model and Dimensional Reduction . . .	57
B.2	Extracting the Screening Masses from the Propagators	61
B.3	The Dependence of the Screening Masses on the Choice of the Temperature Scale and Lattice Spacing	62
C	Self-energy Contributions in 3d fundamental + adjoint Higgs model	64

1 Introduction

According to the standard cosmological model after the Big-Bang the density and the temperature of the early Universe were very high and it consisted actually of a plasma of different elementary particles. This fact is a great opportunity for particle physics since the early Universe thus serves as a laboratory for particle physics. In order to describe the matter under such extreme conditions a new formalism has been developed in the past 25 years which is nowadays called *finite temperature quantum field theory* (see Refs. [1, 2] for detailed monographies on the subject).

As the expanding Universe was cooling down it underwent several phase transitions. Two of these phase transitions, namely the *electroweak phase transition* (EWPT), which occurred when the temperature was $T \sim 200\text{GeV}$ and the *QCD deconfinement phase transition*, which happened at temperature $T \sim 200\text{MeV}$ are of special interest. The underlying theories are well established theoretically and tested experimentally¹. The neighborhood of EWPT is relevant for the understanding the evolution of the baryon asymmetry of the Universe (see [3, 4] for reviews). The theoretical study of QCD deconfinement phase transition is of great practical interest because there is a hope to create *quark-gluon plasma* in relativistic heavy ion collisions. Actually, the possibility of producing the quark-gluon plasma state experimentally was one of the main motivations for detailed studies of this phase transition. One may hope to suggest signals of its existence which can be tested experimentally and to measure some of the thermodynamical properties of the new phase which can be confronted with the expectations based on theoretical models.

One of the most natural signatures of the deconfined phase is the screening of static chromoelectric fields. Actually this was the first signature based on which the existence of the new phase was proven theoretically [5, 6]. More precisely in the confined phase the potential between heavy quark-antiquark pair rises linearly with the distance while in the deconfined phase this potential is exponentially screened, with an inverse screening length equal to the Debye screening mass. The screening of static chromoelectric fields is also of great phenomenological interest in detecting the quark-gluon plasma [7, 8].

In the ideal case when the temperature is sufficiently high the perturbative approach seems to be adequate. The coupling constant is small as the consequence of asymptotic freedom : at high temperature the only scale which is available is the temperature scale itself. The coupling constant is small at large temperature T : $g(T) \sim 1/\ln(T/\Lambda_{QCD})$. Thus naively one would think that the quark-gluon plasma is close to the ideal gas of quarks and gluons (the situation is similar for the high temperature electroweak plasma). However, this simple picture is spoiled by infrared divergencies. It turns out that beyond the natural length scale $1/T$ there are different screening length scales, namely the electric, or the Debye scale $1/gT$ and the magnetic length scale $1/g^2T$. While the electric scale is similar to some extent to the Debye screening scale of QED plasma the magnetic scale is present only in the non-Abelian case. Over the past few years important progress has been made in our understanding of the role of these scales [9, 10, 12, 13, 14]. Electric screening scale is very important in phenomenological investigation of the thermodynamics of the quark-gluon plasma and calculating the signals of the existence of this state [15, 16]. The existence of

¹ The Higgs particle is not yet discovered and supersymmetric extensions of the electroweak theory might be relevant

the electric screening scale sets the boundary of applicability of the naive perturbative approach and provides a possibility to cure some infrared divergencies and to perform a consistent resummation of the perturbative series [9, 13]. In the non-Abelian gauge theory there are, however, also infrared divergencies due to the presence of the magnetic mass scale. This leads to the breakdown of the perturbative approach beyond some order of perturbation theory [17]. It is believed that the existence of the magnetic mass scale is responsible for the termination of the 1st order phase transition in the electroweak theory. This occurs when the Higgs mass is larger than some critical value [18].

In the calculation of static properties at high temperature the most efficient way to deal with the presence of different length scales is the procedure of gradual reduction of the theory [22, 23, 24]². In the past few years considerable progress has been made in understanding the electroweak phase transition based on this approach [10, 11, 12, 19, 21] (see Ref.[4] for a review). Dimensional reduction was also successfully applied to the deconfined phase of QCD [25, 26, 27, 28]. The dimensionally reduced QCD was used for non-perturbative definition of the chromoelectric screening [29, 30]. However, more recent investigations revealed some problems in application of the dimensional reduction in QCD [34].

The present thesis is the comprehensive summary of my work devoted to the investigation of field theoretical screening phenomena by resummation of perturbative series and lattice Monte-Carlo technique. Also I have examined the consistency and precision of dimensional reduction. The organisation of the presented thesis is the following. In section 2 I am going to review the present status of chromoelectric and chromomagnetic screening and their applications to high temperature non-Abelian theories. Section 3 devoted to the self-consistent determination of the screening masses of hot SU(N) gauge theories. In section 4 the validity of dimensional reduction is carefully examined and the screening masses are defined by non-perturbative (lattice Monte-Carlo) technique. In section 5 the screening masses of SU(2) Higgs model will be examined and a new procedure for improving upon the standard of dimensional reduction will be proposed.

Sections 3, 4 and 5 contain the results obtained by the author in collaboration with F. Karsch, M. Oevers, A. Patkós and Zs. Szép.

²The gradual reduction approach is based on integrating out consecutively the heavy fields in the Euclidean path integral. In the first step the non-zero Matsubara modes with typical mass $\sim \pi T$ are integrated out leaving an effective 3d theory. Therefore this approach is also referred to as dimensional reduction. For small enough couplings further reduction is possible by integrating out the static A_0 field (temporal component of the gauge field) with a mass $\sim gT$.

2 Review of non-Abelian Screening

In this section a detailed review of non-Abelian screening phenomenon will be given. The first subsection deals with definition of non-Abelian Debye screening at leading order of perturbation theory. Also a nice physical picture for the non-Abelian chromoelectric screening will be given there. In the following subsections we will discuss infrared problems of finite temperature gauge theories and will introduce the idea of dimensional reduction. Finally, the problem of chromoelectric screening beyond the leading order of perturbation theory will be reviewed.

2.1 Chromoelectric Screening at Leading Order

2.1.1 Chromoelectric Screening in Linear Response Theory

The phenomenon of chromoelectric screening could be easily understood as the field induced by static colour source placed into the plasma. First let us study the response of the plasma to an arbitrary weak external field. The classical source which induces this field is j_{cl}^μ . The perturbation induced by this source is

$$V = \int d^3x j_{cl}^\mu \hat{A}_\mu(x) \quad (1)$$

The classical field induced by this external source is [2]

$$A_\mu(x) = \langle \hat{A}_\mu(x) \rangle = -i \int d^3x' D_{\mu\nu}^R(x-x') j_{cl}^\nu(x), \quad (2)$$

where $D_{\mu\nu}^R(x-x')$ is the retarded gluon propagator. In the momentum representation the retarded gluon propagator could be written as [2]

$$D_{\mu\nu}^R = \frac{i}{K^2 - \Pi_T(K)} P_{\mu\nu}^T + \frac{i}{K^2 - \Pi_L(K)} P_{\mu\nu}^L - i\xi \frac{K_\mu K_\nu}{K^4}, \quad (3)$$

where the following projectors were introduced

$$P_{\mu\nu}^T(K) = \delta_\mu^i (\delta_{ij} - \frac{k_i k_j}{k^2}) \delta_\nu^j, \quad (4)$$

$$P_{\mu\nu}^L(K) = (\delta_{\mu\nu} - \frac{K_\mu K_\nu}{K^2}) - P_{\mu\nu}^T. \quad (5)$$

In the case of static chromoelectric source $J^\mu(x) = Q \delta_0^\mu \delta^3(\mathbf{x})$ the induced potential is

$$\Phi(r) = Q \int \frac{d^3k}{(2\pi)^3} \frac{e^{i\mathbf{k}\cdot\mathbf{x}}}{k^2 + \Pi_L(k_0=0, \mathbf{k})} = \quad (6)$$

$$= \frac{Q}{2\pi^2} \int_{-\infty}^{\infty} \frac{e^{ikr} - e^{-ikr}}{2ir} \frac{k dk}{k^2 + \Pi_L(0, k)}. \quad (7)$$

At leading order in the high temperature limit

$$\Pi_L(k_0 = 0, k) = \Pi_{00}(k_0 = 0, k) = \frac{1}{3}(N + N_f/2)g^2T^2 = m_{D0}^2. \quad (8)$$

for $SU(N)$ and N_f fermion flavour. Now Eq. (8) could be easily evaluated by closing the contour in the upper and lower half complex k -plane and picking up contribution from simple poles at $k = \pm im_{D0}$, which yields

$$\Phi(r) = \frac{Q}{4\pi r} e^{-m_{D0}r}. \quad (9)$$

Thus we can see that the field induced by static colour charge in the plasma is described by screened Coulomb potential. This phenomenon is called chromoelectric or Debye screening³ and the corresponding inverse screening length is called the Debye mass.

2.1.2 Debye screening from classical kinetic theory

The leading order Debye screening mass is determined by the high temperature limit of the one-loop self energy diagram. It was shown that the contribution of such diagrams, the so-called hard thermal loop can be described by an effective kinetic theory [35]. Moreover a simple classical kinetic description could be given for the associated phenomena [36]. The idea of the classical kinetic description is the following.

The large momentum modes ($p \gtrsim T$) of the gauge and fermion fields are described as classical particles with some one-particle distributions. If there are no external fields all particles have equilibrium distributions. If one applies a weak external field to the plasma, the one-particle distributions change and induced currents appear which are proportional to the change of the on-particle distributions. The induced currents create some classical field which is the response of the plasma to external perturbation. This idea should be worked out self-consistently. For this it is necessary to write down the equations of motion for the set of dynamical variables which in non-Abelian case are x^μ , p^μ and Q^a , where Q^a is the classical colour charge. Unlike in Abelian theory here the colour charge Q^a is also subject to dynamical evolution if particles interact with external field. The corresponding equations of motion are [37]

$$m \frac{dx^\mu}{d\tau} = p^\mu, \quad (10)$$

$$m \frac{dp^\mu}{d\tau} = gQ^a F_a^{\mu\nu} p_\nu, \quad (11)$$

$$m \frac{dQ^a}{d\tau} = -gf^{abc} p^\mu A_\mu^b Q^c. \quad (12)$$

Now we can write the collisionless relativistic Boltzmann equation for the one-particle distribution $f_i(x, p, Q)$ for the i -th type of particle:

$$p^\mu \left(\frac{\partial}{\partial x^\mu} - gQ_a F_{\mu\nu}^a \frac{\partial}{\partial p_\nu} - gf_{abc} A_\mu^b Q^c \frac{\partial}{\partial Q_a} \right) f_i(x, p, Q) = 0. \quad (13)$$

³Analogous phenomenon is well known for the electron plasma

If the external field and the gauge coupling are small the distribution f can be expanded in powers of g

$$f = f^{(0)} + gf^{(1)} + \dots, \quad (14)$$

where $f^{(0)}$ is the thermal equilibrium distribution function. The induced current which arises due to the departure from equilibrium is

$$J_a^\mu = g^2 \sum_i \int dP dQ p^\mu f_i^{(1)}(x, p, Q) Q_a, \quad (15)$$

where summation stands for all species of particles which are present in the plasma. From Eq. (13) one finds [36]

$$f^{(1)} = Q_a \left[A_0^a(x) - \frac{p_\mu}{p \cdot \partial} \partial_0 A_\mu^a(x) \right] \frac{df_i^{(0)}}{dp_0} \quad (16)$$

and the induced current can be written as

$$J_a^\mu = g^2 \sum_i \int dP dQ p^\mu Q_a Q_b \left(A_0^b(x) - \frac{p^\nu}{p \cdot \partial} \partial_0 A_\nu^b(x) \right) \frac{df_i^{(0)}}{dp_0}. \quad (17)$$

If one takes into account that

$$dP = \frac{d^4 p}{(2\pi)^4} 2\theta(p_0) \delta(p^2 - m^2) \quad (18)$$

and

$$\int dQ Q^a Q^b = \begin{cases} N \delta^{ab}, & \text{for gluons} \\ \frac{1}{2} \delta^{ab}, & \text{for quarks} \end{cases} \quad (19)$$

one arrives at the following expression for the induced current

$$J_a^\mu(x) = m_{D0}^2 \int \frac{d\Omega}{4\pi} v^\mu i \left(\frac{v_\nu}{v \cdot \partial} \partial_0 A_\nu^a(x) - A_a^0(x) \right), \quad (20)$$

where $v = (1, \hat{\mathbf{p}})$, $\hat{\mathbf{p}} = \mathbf{p}/|\mathbf{p}|$ and $m_{D0}^2 = 1/3g^2T^2(N + 1/2N_f)$ for N_f fermion flavours. For static fields the above expression simply reduces to

$$J_a^\mu(x) = -m_{D0}^2 A_a^0(\mathbf{x}) \delta_0^\mu. \quad (21)$$

If this expression is inserted to the corresponding field equation the screened Coulomb potential is easily recovered.

2.1.3 Polyakov Loop Correlator and the Debye Screening

Quantities which characterize the phases of a gauge theory are the free energies of static configurations of quarks and antiquarks. Following Ref. [6] let us introduce operators, $\psi_a^\dagger(\mathbf{r}_i, t)$ and $\psi_a(\mathbf{r}_i, t)$, which create and annihilate static quarks with colour a at position \mathbf{r}_i

and time t , along with their conjugates $\psi_a^{\dagger c}$ and ψ_a^c for antiquarks. These static fields satisfy equal time anticommutation relations

$$[\psi_a(\mathbf{r}_i, t), \psi_b^{\dagger}(\mathbf{r}_j, t)]_+ = \delta_{ij} \delta_{ab} \quad (22)$$

The evolution equation for the static quark fields is

$$\left(\frac{1}{i} \frac{\partial}{\partial t} - \vec{\tau} \cdot \vec{A}_0(\mathbf{r}_i, t) \right) \psi(\mathbf{r}_i, t) = 0, \quad (23)$$

where $\vec{\tau} \cdot \vec{A}_0 = \tau^a A_0^a$ with τ^a being the generators of SU(N) gauge group. The above equation may be formally integrated to yield

$$\psi(\mathbf{r}_i, t) = T \exp \left(i \int_0^t \vec{\tau} \cdot \vec{A}_0(\mathbf{r}_i, t) \right) \psi(\mathbf{r}_i, 0) \quad (24)$$

The free energy of a configuration of N_q quarks and $N_{\bar{q}}$ at positions $\mathbf{r}_1, \dots, \mathbf{r}_{N_q}$ and $\mathbf{r}'_1, \dots, \mathbf{r}'_{N_{\bar{q}}}$

$$\exp(-\beta F(\mathbf{r}_1, \dots, \mathbf{r}_{N_q}, \mathbf{r}'_1, \dots, \mathbf{r}'_{N_{\bar{q}}})) = \frac{1}{N^{N_q+N_{\bar{q}}}} \sum_s \langle s | e^{-\beta H} | s \rangle, \quad (25)$$

with summation over all states with heavy quarks at $\mathbf{r}_1, \dots, \mathbf{r}_{N_q}$ and antiquarks at $\mathbf{r}'_1, \dots, \mathbf{r}'_{N_{\bar{q}}}$, $\beta = T^{-1}$ and N being the dimension of the SU(N) algebra. The above expression could be rewritten as

$$\begin{aligned} & \exp(-\beta F_{N_q, N_{\bar{q}}}) = \\ & = \frac{1}{N^{N_q+N_{\bar{q}}}} \sum_{s'} \langle s' | \sum_{(ab)} \psi_{a_1}(\mathbf{r}_1, 0) \dots \psi_{a_{N_q}}(\mathbf{r}_{N_q}, 0) \psi_{b_1}^c(\mathbf{r}'_1, 0) \dots \psi_{b_{N_{\bar{q}}}}^c(\mathbf{r}'_{N_{\bar{q}}}, 0) \\ & \times e^{-\beta H} \psi_{a_1}^{\dagger}(\mathbf{r}_1, 0) \dots \psi_{a_{N_q}}^{\dagger}(\mathbf{r}_{N_q}, 0) \psi_{b_1}^{\dagger c}(\mathbf{r}'_1, 0) \dots \psi_{b_{N_{\bar{q}}}}^{\dagger c}(\mathbf{r}'_{N_{\bar{q}}}, 0) | s' \rangle, \end{aligned} \quad (26)$$

where now the sum is over all states with no heavy quarks. Since $e^{-\beta H}$ generates Euclidian time translations, i.e. $e^{\beta H} \hat{O}(t) e^{-\beta H} = \hat{O}(t + \beta)$ for any operator, (26) becomes

$$\begin{aligned} & \exp(-\beta F_{N_q, N_{\bar{q}}}) = \\ & = \frac{1}{N^{N_q+N_{\bar{q}}}} \sum_{s'} \langle s' | \sum_{(ab)} e^{-\beta H} \psi_{a_1}(\mathbf{r}_1, \beta) \psi_{a_1}^{\dagger}(\mathbf{r}_1, 0) \dots \psi_{a_{N_q}}(\mathbf{r}_{N_q}, \beta) \psi_{a_{N_q}}^{\dagger}(\mathbf{r}_{N_q}, 0) \\ & \times \psi_{b_1}(\mathbf{r}'_1, \beta) \psi_{b_1}^{\dagger}(\mathbf{r}'_1, 0) \dots \psi_{b_{N_{\bar{q}}}}(\mathbf{r}'_{N_{\bar{q}}}, \beta) \psi_{b_{N_{\bar{q}}}}^{\dagger}(\mathbf{r}'_{N_{\bar{q}}}, 0) | s' \rangle \end{aligned} \quad (27)$$

Using (24) and (22) and introducing the Polyakov loop ⁴

$$L(\mathbf{r}) = \frac{1}{N} \text{Tr} P \exp \left(i \int_0^{\beta} dt \vec{\tau} \cdot \vec{A}_0(\mathbf{r}, t) \right), \quad (28)$$

(27) becomes

$$\exp(-\beta F_{N_q, N_{\bar{q}}}) = \text{Tr} \left[e^{-\beta H} L(\mathbf{r}_1) \dots L(\mathbf{r}_{N_q}) L^{\dagger}(\mathbf{r}'_1) \dots L^{\dagger}(\mathbf{r}'_{N_{\bar{q}}}) \right] \quad (29)$$

⁴This object is also referred to as Wilson line.

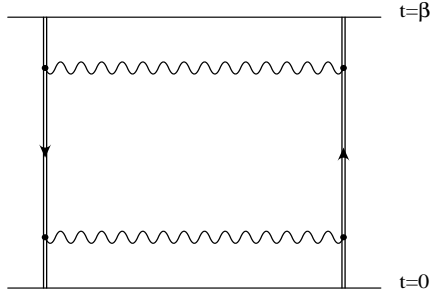


Figure 1: Two gluon contribution to the Polyakov loop correlation function

Let us consider the simplest case of an quark-antiquark pair at distance \mathbf{r} from each other. In this case the additional free energy due to presence of this pair is simply given by the Polyakov loop correlator

$$\exp(-\beta F_{q\bar{q}}) = \langle L(\mathbf{r})L^\dagger(0) \rangle, \quad (30)$$

where $\langle .. \rangle$ denotes thermal average over the gluon configurations. The Polyakov loop has following nice properties. First, it is gauge invariant because the gauge field is periodic in time $A_\mu(\mathbf{r}, 0) = A_\mu(\mathbf{r}, \beta)$, second, its definition on lattice is straightforward

$$L(\mathbf{r}) = \frac{1}{N} \text{Tr} \prod_{i=1}^{N_t} U^0(\mathbf{r}, t), \quad (31)$$

where N_t is the extension of the lattice in temporal direction. In the confined phase ($T < T_c$ with T_c being the temperature of the deconfinement phase transition) the large distance behavior of the Polyakov loop correlator is the following [5]

$$\langle L(\mathbf{r})L^\dagger(0) \rangle = \exp(-\sigma(T)|\mathbf{r}|/T) \quad (32)$$

implying confinement. In the deconfined phase at very high temperature (small coupling) the dominant contribution to the Polyakov loop correlators is given by the exchange of two screened electric gluons (see Figure 1). Calculation of the corresponding diagram yields

$$\langle L(\mathbf{r})L^\dagger(0) \rangle = \exp(-V(|\mathbf{r}|)/T), \quad (33)$$

with

$$V(r) = \frac{N^2 - 1}{8N^2} \left(\frac{g^2}{4\pi r} \right)^2 e^{-2m_{D0}r}. \quad (34)$$

Thus the screening mass determined from the Polyakov loop correlators is twice the Debye mass, $M_D = 2m_{D0}$. From definition of $V(r) \equiv F_{q\bar{q}}$ it is obvious that it is a thermal average over $q\bar{q}$ potentials in the possible colour channels. Let us consider the simplest case of $SU(2)$ gauge group. In this case the free energy of quark-antiquark pair (which is often referred to as colour averaged potential) can be written as

$$e^{-\beta V(r)} = \frac{1}{4} (e^{-\beta V_1(r)} + 3e^{-\beta V_3(r)}) \quad (35)$$

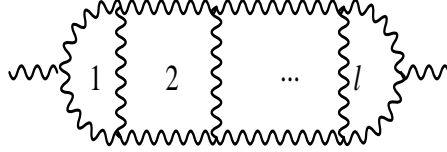


Figure 2: Divergent l -loop contribution to the 2-point function

where $V_1(V_3)$ denotes the $q\bar{q}$ potential in the singlet (triplet) channel for two isospin $\frac{1}{2}$ particles. These potentials can be calculated perturbatively and contrary to $V(r)$ they are dominated by one gluon exchange. The corresponding calculation yields [6]

$$V_i(r) = c_i g^2 \frac{1}{4\pi r} e^{-m_{D_0} r}, \quad (36)$$

with $c_1 = -3/4$ and $c_3 = 1/4$. At high temperature g^2 is small and one may expand the exponentials in (35) and verify that the $\mathcal{O}(g^2)$ terms cancel between singlet and triplet terms yielding Eq. (34) for V .

2.2 Infrared divergencies Associated with Static non-Abelian Magnetic Fields

The application of the naive perturbation theory at finite temperature is obstructed by infrared divergencies of thermal field theory. In scalar field theory and in abelian gauge theory these IR problems can be cured by appropriate resummations which take into account the presence of the screening scale gT (see [1, 2] and also discussion in section 2.5). In non-Abelian gauge theories, however, there exists also another sort of IR problems associated with static magnetic fields [17]. Static magnetic fields are not screened at leading order of perturbation theory: the IR limit of the 1-loop transverse self-energy vanishes in all gauges.

Let us consider a generic l -loop contribution to the self-energy which is shown in Figure 2. To evaluate the leading infrared divergent contribution we can assume that all propagators in Figure 2 are static, i.e. consider only contribution from zero Matsubara modes. In this case neglecting all tensorial structures the contribution of these diagram is

$$\underbrace{g^{2l}}_{\text{vertex}} \underbrace{\left(\int d^3p \right)^l}_{\text{loop integral}} \underbrace{p^{2l}}_{\text{vertex}} \underbrace{(p^2 + m^2)^{-3l+1}}_{\text{propagators}}. \quad (37)$$

In the above expression we have introduced a magnetic mass since one might expect that such a mass scale is generated by higher loop contribution. Using simple power counting arguments one can see that for $l = 2$ the corresponding contribution is

$$g^4 T^2 \ln \frac{T}{m} \quad (38)$$

and for $l \geq 3$ one has

$$g^4 T^2 \left(\frac{g^2 T}{m} \right)^{l-2} \quad (39)$$

Since no magnetic mass is generated at 1-loop level it is natural to assume $m \sim g^2 T$. In this case as one can see from Eq. 39, infinite number of diagrams contribute to g^4 order self-energy. If m is proportional to the power of g , higher than 2 no weak coupling expansion could be obtained. However, as we will see in the next section the magnetic mass turns out to be of order $g^2 T$. Different approaches for determination of the numerical value of the magnetic mass will be discussed in sections 3 and 4.

An analysis of the higher loop diagrams similar to that presented above shows that $\mathcal{O}(g^6)$ contribution to the weak coupling expansion of the free energy is non-perturbative. Let us emphasize that the Linde's conjecture does not imply that no weak coupling expansion is possible in finite temperature non-abelian gauge theory. It just states that beyond some order the coefficients of the weak coupling expansion cannot be evaluated by calculating finite numbers of Feynman diagrams. In fact the coefficient of the term proportional to the weak coupling expansion of the free energy was calculated by lattice Monte-Carlo technique [38]. Linde's conjecture also implies as we will see in subsection 2.3 that the next-to-leading contribution to the Debye mass is non-perturbative.

2.3 Dimensional reduction

Finite temperature field theories exist in a volume with one compact dimension, the imaginary time, and the appropriate boundary conditions [1, 2]. The extension of the compact dimension is $\beta = T^{-1}$. At high temperature this dimension becomes arbitrary small. Therefore the degrees of freedom in time direction are essentially frozen. This situation can be also viewed differently. Consider the Yang-Mills action at finite temperature

$$S = \int_0^\beta dt \int d^3x \frac{1}{4} F_{\mu\nu}^a F_{\mu\nu}^a \quad (40)$$

The 4-dimensional gauge field $A_\mu^a(t, \mathbf{x})$ can be written in terms of an infinite set of 3-dimensional fields using Matsubara decomposition

$$A_\mu^a(t, \mathbf{x}) = \sqrt{T} \sum_{n=-\infty}^{\infty} e^{i\omega_n t} A_{\mu n}^a(\mathbf{x}), \quad \omega_n = 2\pi T \quad (41)$$

From this expression it is clear that all modes with $n \neq 0$ have a mass $2\pi T n$. In $T \rightarrow \infty$ limit these modes become infinitely heavy and according to conventional wisdom based on Appelquist-Carrazone theorem these will decouple [39]. Thus the Yang-Mills action reduces to an action containing only static fields of the following form

$$S = \int d^3x \left(\frac{1}{4} F_{ij}^a F_{ij}^a + \frac{1}{2} (D_i A_0^a)^2 \right), \quad (42)$$

with

$$D_i A_0^a = \partial_i A_0^a - g_3 f^{abc} A_0^b A_i^c \quad (43)$$

$$F_{ij}^a = \partial_i A_j^a - \partial_j A_i^a + g_3 f^{abc} A_i^b A_j^c \quad (44)$$

$$g_3^2 = g^2 T. \quad (45)$$

This is the action of the 3 dimensional gauge theory which interacts with an Euclidian scalar and isovector field A_0 . This matter field originates from the time component of the original Yang-Mills field. In more careful analysis where non-static modes are integrated out at 1-loop level it has been shown that a mass term and quartic self-interaction is generated for the A_0 field [24]. Thus the effective action describing the dynamics of zero modes assumes the form

$$S = \int d^3x \left(\frac{1}{4} F_{ij}^a F_{ij}^a + \frac{1}{2} (D_i A_0^a)^2 + \frac{1}{2} m_{D0}^2 A_0^a A_0^a + \lambda_A (A_0^a A_0^a)^2 \right), \quad (46)$$

where

$$m_{D0}^2 = \frac{1}{3} g^2 T^2 (N + \frac{1}{2} N_f) \quad (47)$$

is the leading order Debye mass and

$$\lambda_A = (6 + N - N_f) \frac{g^4 T}{96\pi^2} \quad (48)$$

with N_f being the number of fermion flavours [24, 34]. In Ref. [34] integration of non-static modes was performed at 2-loop level and it turned out that the 2-loop corrections to the parameters g_3^2 , m_{D0} and λ_A are small. Higher dimensional and non-local operators are also generated by 1-loop integration of non-static modes, however, we have neglected this operators because their coefficients vanish in $T \rightarrow \infty$ limit. The impact of higher dimensional operators was analyzed in Ref. [10] and non-local operators were studied in Ref. [40]. Let us note that naive decoupling of non-static modes does not take place because the effective mass and quartic vertex generated by integration of non-static modes does not vanish in $T \rightarrow \infty$ limit. If the temperature is sufficiently high, $g_3^2 \ll m_{D0}$ i.e. the A_0 field becomes very heavy and can be also integrated out. The effective theory obtained by integrating out the A_0 field is the 3 dimensional Yang-Mills theory

$$S_{YM3} = \int d^3x \frac{1}{4} F_{ij}^a F_{ij}^a \quad (49)$$

This theory is superrenormalizable and therefore the only dimensionfull scale in the theory is g_3^2 . This is the reason why the magnetic mass is expected to be proportional to $g_3^2 = g^2 T$. Both the 3 dimensional Yang-Mills and the adjoint SU(N) Higgs models are confining theories, thus we can see that the infrared problems of finite temperature non-abelian gauge theory are related to the physics of 3d confinement.

2.4 The Non-Abelian Debye Screening beyond Leading Order

2.4.1 Non-Abelian Debye Screening in One-Loop Resummed Perturbation Theory and the Magnetic Mass

The next-to-leading correction to Π_L is of order g^3 and arises from summation of ring diagrams [1]. The summation of ring diagrams simply amounts to replacing the bare propagator with the 1-loop resummed propagator and evaluating the 1-loop diagram with the resummed propagator. The natural candidate for next-to-leading Debye mass would be

$\Pi_L(k_0 = 0, k \rightarrow 0)$. However, this quantity is gauge dependent [41]. We have seen in section 2.1 that the Debye screening arises from poles $k = \pm im_{D0}$ in the gluon propagator. Therefore the natural extension of the Debye screening mass is

$$m_D^2 = \Pi_L(k_0 = 0, k^2 = -m_D^2). \quad (50)$$

This definition will lead to gauge invariant result because the pole of the propagator was proven to be gauge independent at each order of perturbation theory [42]. $\Pi_L(k_0 = 0, k)$ was calculated in 1-loop resummed perturbation theory in the high temperature limit in Ref. [43] and it turns out that $k^2 = -m_D^2$ is a starting point of branch cut rather than a pole. This fact would mean a non-exponential anomalous screening. If one introduces the magnetic mass m_T , i.e. replaces the static massless magnetic propagators with massive ones the next-to-leading result for Π_L in R_ξ gauge reads [43]

$$\begin{aligned} \Pi_L(k_0, k) = & \frac{g^2 T N}{4\pi} \left[-m_D - m_T \right. \\ & + \frac{2m_D^2 - 2k^2 - m_T^2}{k} \arctan \frac{k}{m_D + m_T} + \\ & (k^2 + m_D^2) \left(\frac{k^2 + m_D^2}{m_T^2 k} \left(\arctan \frac{k}{m_D + \sqrt{\xi} m_T} - \arctan \frac{k}{m_D + m_T} \right) + \right. \\ & \left. \left. \left(\sqrt{\xi} - 1 \right) \frac{1}{m_T} \right) \right] \end{aligned} \quad (51)$$

As one can see from this expression Π_L has gauge invariant poles at $k = \pm im_D$ and the starting point of the branch cut has been shifted to $k = i(m_D + m_T)$. Thus the exponential nature of the screening is restored. As far as one is interested in obtaining the weak coupling expansion of the Debye mass, m_D should be replaced by m_{D0} on the rhs. of equation (50). Then the next-to-leading correction for the Debye mass reads

$$m_{D1}^2 - m_{D0}^2 = \frac{Ng^2 T}{2\pi} m_{D0} \left[\left(1 - \frac{m_T^2}{4m_{D0}^2}\right) \ln \frac{2m_{D0} + m_T}{m_T} - \frac{1}{2} - \frac{m_T}{2m_{D0}} \right]. \quad (52)$$

Thus we can see that the value of the Debye mass at next-to-leading order is strongly influenced by the magnetic mass. An alternative possibility which will be considered in section 3 is a self-consistent determination of m_D from the equation (50), which is equivalent diagrammatically to a summation of "super-daisy" diagrams [44]. Analogously to the Debye mass the magnetic screening mass can be defined as

$$m_T^2 = \Pi_T(k_0 = 0, k^2 = -m_T^2), \quad (53)$$

where Π_T is defined by equation (3). Though the pole of the transverse gluon propagator is called magnetic screening mass its relation to the screening of static magnetic fields is not obvious. The magnetic screening could be defined in terms of the free energy of monopole-antimonopole pair ⁵. However, it cannot be stated that for the weak coupling

⁵The divergence of the static non-Abelian magnetic field is non-zero because the the corresponding non-Abelian field equation is $\nabla \cdot \mathbf{B}^a = g f^{abc} \mathbf{A}^b \cdot \mathbf{B}^c$. Therefore there may exist non-Abelian field configurations which act as magnetic monopoles

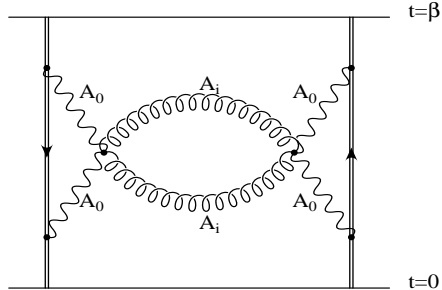


Figure 3: Contribution of magnetic gluons to the Polyakov loop correlation function

regime this energy is dominated by exchange of a static transverse gluon. Because of the Linde's conjecture all multi gluon exchange have to be considered.

The magnetic screening can be defined by studying the large distance behaviour of the field created by a magnetic monopole. This was realized on lattice investigations [45, 46] by calculating the magnetic flux leaving the spatial 3d cube and also by semiclassical approximation by Bíró and Müller [47]. In the lattice investigation the corresponding inverse screening length was found to be $0.24g^2T$ [45] and $0.27(3)g^2T$ in Ref. [46]. The semiclassical approach of Ref. [47] yields the result $0.25g^2T$ which is consistent with the previous ones. From the arguments given above it is clear, however, that this inverse screening length cannot be directly related to the magnetic mass defined from the propagator.

2.4.2 Non-Perturbative definitions of the Debye mass

We are interested in definitions of the Debye mass which do not rely on perturbation theory and can be easily implemented in lattice Monte-Carlo simulations. A natural way to determine the Debye screening mass non-perturbatively is to measure the gluon propagator on lattice. Such measurement were done in Refs. [48, 49] in finite temperature 4d SU(2) gauge theory and also in 3d effective theory in Ref. [50]. We will discuss the non-perturbative determination of the propagators in section 4 in detail.

Let us consider the Polyakov loop correlator which is a manifestly gauge invariant quantity. At leading order the Polyakov loop correlator is determined by the exchange of two electrostatic gluons as shown in Figure 2 (see subsection 2.1.3) leading to exponential screening with the inverse screening length equal to $2m_{D0}$.

Beyond leading order, however, Polyakov loops can also couple to magnetostatic gluons as shown in Figure 3. At high temperatures different mass scales which are present in the plasma are separated $2\pi T \gg gT \gg g^2T$ due to asymptotic freedom. Then the infrared problems associated with static magnetic fields are related to the physics of 3 dimensional confinement. Because of the 3 dimensional confinement Polyakov loops cannot exchange a pair of magnetic gluons, the pair will instead form a glueball with a mass of order $g_3^2 = g^2T$. Thus the large distance behaviour of the Polyakov loop correlators will be determined by the lightest glueball state of the 3 dimensional Yang-Mills theory [51, 52]. Thus the true large distance behaviour of Polyakov loop correlator at very high temperature has nothing to do with the physics of the Debye screening.

For vectorially coupled theories (like QCD at zero chemical potential but not the elec-

trweak theory) an alternative non-perturbative definition of the Debye mass was suggested by Arnold and Yaffe [29] This definition relies on the fact that in vectorially-coupled theories at finite temperature there is a symmetry, namely the Euclidian time reflection symmetry that excludes the unwanted exchange of pairs of magnetostatic gluons. The crucial property is that the temporal component of the gauge field A_0 is odd under this symmetry while the spatial gauge field A_i is even. Thus non-perturbatively the Debye mass can be associated with a correlation function of some gauge invariant operator which is odd under Euclidian time reflection and which has the largest correlation length. Some gauge invariant time-reflection odd operators are listed in Ref. [29]. As far as one is interested in the leading non-perturbative correction i.e. the coefficient of the $g^2 \ln g$ and g^2 terms in

$$m_D = m_{D0} + c_1 g^2 \ln g + c_2 g^2 + \dots \quad (54)$$

it is not necessary to calculate correlation function in the full 4 dimensional theory. One can instead consider the effective theory, construct the corresponding operators and measure their correlation function there. Various realisation of this strategy have been recently discussed in the literature [30, 31, 32, 33].

2.5 Screened Perturbation Theory

One of the main motivation for studying the screening masses is their role in the physical expression of different thermodynamic quantities like thermodynamic potentials. The weak coupling expansion of the QCD free energy does show very bad convergence properties [53, 54, 55, 56, 57, 58]. Only in the TeV temperature range can one find a satisfactory numerical convergence rate [59].

Recently, in the case of scalar ϕ^4 theory, where conventional perturbative expansion encounters similar convergence problems, several proposals have been made for new types of perturbative expansion which shows better convergence [60, 61, 62]. The outcome of the resummed perturbative calculation for the free energy density may depend on the correct choice of the screening mass [60, 62].

In Ref. [60] it was shown that the poor convergence of perturbative expansion can be improved if the series expansion is reorganized in loop expansion with screened propagators; i.e. instead of expanding around the free energy density of a massless ideal gas, loop expansion is performed starting from a massive ideal gas ⁶. Following Ref. [60] consider an $O(N)$ symmetric scalar field theory with the following Lagrangian

$$\begin{aligned} L &= L_0 + L_{int}, \\ L_0 &= \frac{1}{2}((\partial\phi_i)^2 + m^2\phi_i^2), \\ L_{int} &= -\frac{1}{2}m^2\phi_i^2 + \frac{g^2}{24N}(\phi_i^2)^2 + \frac{g^2}{24N}(Z_2 - 1)(\phi_i^2)^2. \end{aligned} \quad (55)$$

Following ref. [63, 64] we have introduced and subtracted a mass term with $m \sim \mathcal{O}(g)$ in order to reorganize the perturbative expansion. The coupling constant renormalisation factor is given by [65]

$$Z_2 = 1 + \frac{3g^2}{(4\pi)^2} \frac{N+8}{18\epsilon} + \mathcal{O}(g^4), \quad (56)$$

⁶The propagators become massive by the mechanism of Debye screening generated by the thermal fluctuation in analogous way as in gauge theories.

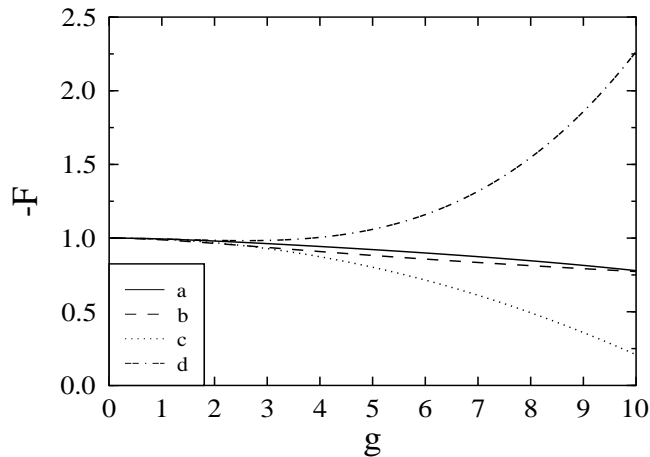


Figure 4: Shown is the free-energy density of the $N=1$ scalar field theory as a function of the scalar self-coupling g in the units of the free energy density of a massless ideal gas ($\frac{\pi^2 T^4}{90}$) (from Ref. [60]). The curves represent 2-loop (a) and 1-loop (b) results of the screened loop expansion as well as the $\mathcal{O}(g^2)$ (c) and $\mathcal{O}(g^3)$ (d) results of the conventional perturbative expansion.

and we have neglected the field renormalisation factor Z_1 , which is unity up to $\mathcal{O}(g^4)$.

The free energy can be easily evaluated with massive propagators up to 2-loop, but in the limit of large N also the 3-loop contribution can be evaluated. The details of the calculation can be found in Ref. [60]. To evaluate the free energy numerically the screening mass has to be specified. It turns out that the final result is sensitive to the actual value of the screening mass [66]. The most natural way of the determination of the screening mass is the use of a 1-loop gap equation [44, 67, 68], which for our case reads ⁷

$$m^2 = \frac{g^2(N+2)}{6N} \left(I(m) + \frac{m^2}{16\pi^2} \left(\frac{1}{\epsilon} + \ln \frac{\bar{\mu}^2}{T^2} \right) \right), \quad (57)$$

with

$$I(m) = \sum_{n=-\infty}^{\infty} \int \frac{d^3p}{(2\pi)^3} \frac{1}{p^2 + \omega_n^2 + m^2}, \quad \omega_n = 2\pi Tn. \quad (58)$$

The numerical results for the free energy density in the case of the $N = 1$ component theory as a function of the self-coupling calculated in the screened perturbation theory is shown in Figure 4. Also shown are the results obtained with the conventional perturbative expansion up to $\mathcal{O}(g^2)$ and $\mathcal{O}(g^3)$ in the scalar self-coupling. The Figure clearly shows that the difference between the 1-loop and 2-loop results of the screened perturbative expansion is small and essentially stays constant over the entire range of couplings. In the conventional perturbative approach, on the other hand, different orders in the expansion differ largely from each other. For large N as it was mentioned above also the 3-loop contribution can be calculated. The corresponding results are shown in Figure 5 for $N = 10$. As one can see from the figure the convergence of the perturbative expansion is substantially improved as compared to the usual perturbative expansion.

Let us notice that an attempt to generalize this approach to the case of QCD have been recently reported in Ref. [69]. The authors were able to find a compact formula for the

⁷In the limit of large N this equation is exact and therefore its solution can also be used in 3-loop calculations. The gap equation should be properly renormalized before it is solved numerically. Therefore a divergent and scale dependent counterterm was added; see discussion in Ref. [62] on this issue.

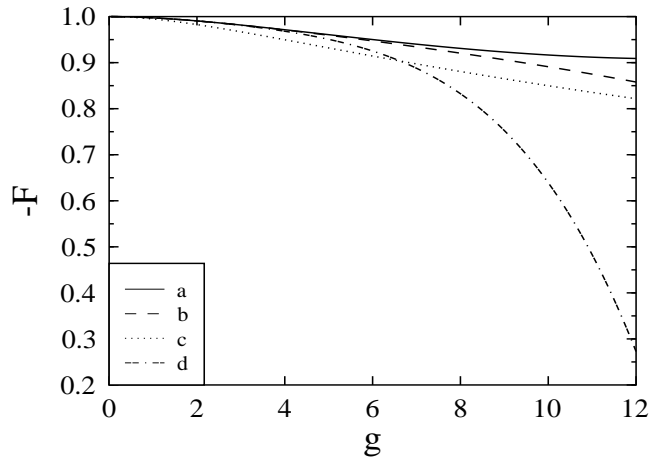


Figure 5: The free energy density of the scalar field theory in the large- N limit as a function of the scalar self-coupling g in units of the free energy density of a massless ideal gas (from Ref [60]). Shown are results for $N = 10$ (see text). The curves represent 3-loop (a) 2-loop (b) and 1-loop (c) results of the screened loop expansion as well as the $\mathcal{O}(g^4)$ (d) results of the conventional perturbative expansion.

leading order massive gas contribution to the free energy density of the hot gluon gas. In distinction to phenomenological approaches [15], their expression also takes into account the contribution of the longitudinal fluctuations and also the effect of Landau-damping appears in addition to the quasiparticle piece of the free energy. The screening mass of the gluons remains a free parameter, which emphasizes the importance of its independent determination.

3 Coupled Gap Equation for the Screening Masses in Hot SU(N) Gauge Theory

As it was discussed in section 2.4 a natural way to calculate the Debye mass is to solve the (gap) equation $m_D^2 = \Pi_L(k_0 = 0, k^2 = -m_D^2)$ in a self-consistent way. This definition is gauge invariant but requires the introduction of the magnetic mass which can be associated with a dynamically generated mass gap of pure 3d gauge theory if the temperature is high enough. The magnetic mass was calculated using self-consistent approach in the effective 3d gauged Higgs and also in 3d pure gauge theories [68, 67, 70, 72, 73]. In the case of the Electroweak Theory (or SU(2) Higgs model) the gauge coupling is small for the temperature range of interest and a hierarchy of the different mass scales holds $2\pi T \gg gT \gg g^2 T$. Due to this fact different screening masses could be determined separately in the corresponding effective theories. In hot SU(N) theory for the temperature range of interest the above hierarchy of scales fails to hold. Therefore we should investigate a coupled set of gap equations for all the screened modes and determine the corresponding screening lengths simultaneously.

The most straightforward way to do this would be to derive gap equations in the full four-dimensional theory. However, it is not known how to generalize the by-now well-established three-dimensional gauge invariant resummation [70, 71, 72, 73] to four dimensions. There are gauge transformations which might mix static and non-static modes, therefore the resummation of the static modes only, which was suggested in [74] violates gauge invariance. Since screening masses are static quantities it is natural to calculate them in the framework of an effective three-dimensional theory which is, however, valid only up to scales $k \lesssim gT$. It was shown that the accuracy of the description of such theories is improved if in the action of the effective theory besides superrenormalizable operators one also takes into account higher dimensional and non-local operators [75, 40].

When deriving the gap equation in the framework of three-dimensional adjoint Higgs model it is important to address the question whether the symmetric or the broken phase is the physical one. Dimensional reduction is valid if $A_0 \ll \sqrt{T}$. However, in the broken phase the expectation value of the A_0 field is $A_0 \sim \frac{1}{g}$. Therefore for small g the broken symmetry phase cannot be the physical one. We will return to this question in section 4, but here we will assume no A_0 background.

In this section we shall assume only the separation of the static and non-static scales in the pure SU(N) gauge theory, that is we assume that $g(T) \ll 2\pi$, and derive different versions of the coupled gap equations in the corresponding effective theory, the 3d adjoint Higgs model. Presentation in this section relies on Ref. [76].

3.1 Gauge non-invariant resummation scheme

This scheme for the evaluation of the magnetic mass was first suggested in [71] and for the Debye mass in [43]. It was noticed in Ref. [71] that magnetic mass obtained in this scheme is gauge dependent and therefore cannot be regarded as physically meaningful. However, even in gauge invariant resummation schemes the value of the magnetic mass cannot be defined unambiguously, because its approximate value depends on the specific resummation scheme [73]. Therefore it is of a certain interest to calculate the magnetic mass even in a gauge non-invariant scheme just to compare the amount of gauge dependence with the

ambiguity of different gauge invariant approaches, when evaluated to leading order is some approximation scheme.

The three-dimensional effective Lagrangian relevant for 1-loop calculations can be written with R_ξ gauge as (see Eq. (46))

$$\begin{aligned}
L &= \frac{1}{4}F_{ij}^a F_{ij}^a + \frac{1}{2} \left((D_i A_0)^2 + m_D^2 A_0^a A_0^a \right) + \\
&\frac{1}{2} m_T^2 A_i^a A_i^a + (\partial_i \bar{c}^a D_i c^a + m_G^2 \bar{c}^a c^a) + \frac{1}{2\xi} (\partial_i A_i)^2 + L_{ct}, \\
L_{ct} &= \frac{1}{2} (m_{D0}^2 - m_D^2) A_0^a A_0^a - \frac{1}{2} m_T^2 A_i^a A_i^a - m_G^2 \bar{c}^a c^a
\end{aligned} \tag{59}$$

Here we have added and subtracted a mass term for A_i , A_0 and the ghost fields (c) with their exact screening masses. m_{D0}^2 is the tree-level (from the point of view of the effective theory) Debye mass for A_0 , which was generated during the procedure of the dimensional reduction and defined by Eq. (47). The propagators can be read from the quadratic part of the Lagrangian and can be found in the Appendix A, where one also finds some details of the evaluation of the relevant Feynman diagrams contributing to the different 2-point functions. It should be noticed when performing the resummation of the pure gauge sector with the unique mass term m_T , the longitudinal and transverse gluons acquire different masses, which are, however related by $m_L = \sqrt{\xi} m_T$ (m_T is the transverse and m_L is the longitudinal mass). It is also possible to perform the resummation by introducing independent masses for the longitudinal and transverse gluons, but then the corresponding gap equations will have only complex solutions. The gauge boson self-energy can be decomposed as

$$\Pi_{ij}(k) = \left(\delta_{ij} - \frac{k_i k_j}{k^2} \right) \Pi_T(k, m_T, m_D, m_G) + \frac{k_i k_j}{k^2} \Pi_L(k, m_T, m_D, m_G). \tag{60}$$

In the Appendix A we give the expression of Π_{ij} in terms of a few fundamental three-dimensional loop-integrals. These integrals are easily evaluated and an explicit but very cumbersome functional form can be written for the longitudinal and transversal projections of the polarisation matrix. The self-energy of the ghost fields is also given in Appendix A.

The self energy for A_0 was first calculated in [43]:

$$\begin{aligned}
\Pi_{00}(k, m_D, m_T) &= m_{D0}^2 + \frac{g^2 N}{4\pi} \left[-m_D - m_T + \frac{2(m_D^2 - k^2 - m_T^2/2)}{k} \arctan \frac{k}{m_D + m_T} \right. \\
&\left. + (k^2 + m_D^2) \left(\frac{k^2 + m_D^2}{m_T^2 k} \left(\arctan \frac{k}{m_D + \sqrt{\xi} m_T} - \arctan \frac{k}{m_D + m_T} \right) + (\sqrt{\xi} - 1) \frac{1}{m_T} \right) \right].
\end{aligned} \tag{61}$$

The above self-energies are functions of the magnitude of momentum but also depend parametrically on the screening masses. The on-shell gap equations now can be written as

$$\begin{aligned}
m_T^2 &= \Pi_T(k^2 = -m_T^2, m_T, m_D, m_G), \\
m_D^2 &= \Pi_{00}(k^2 = -m_D^2, m_D, m_T), \\
m_G^2 &= \Pi_G(k^2 = -m_G^2, m_T, m_G).
\end{aligned} \tag{62}$$

On the mass-shell $\Pi_{00}(k^2 = -m_D^2, m_D, m_T)$ is gauge parameter independent, but $\Pi_T(k^2 = -m_T^2, m_T, m_D, m_G)$ and $\Pi_G(k^2 = -m_G^2, m_T, m_G)$ do depend on the gauge fixing parameter, therefore the masses obtained from this coupled set of gap equations are gauge dependent.

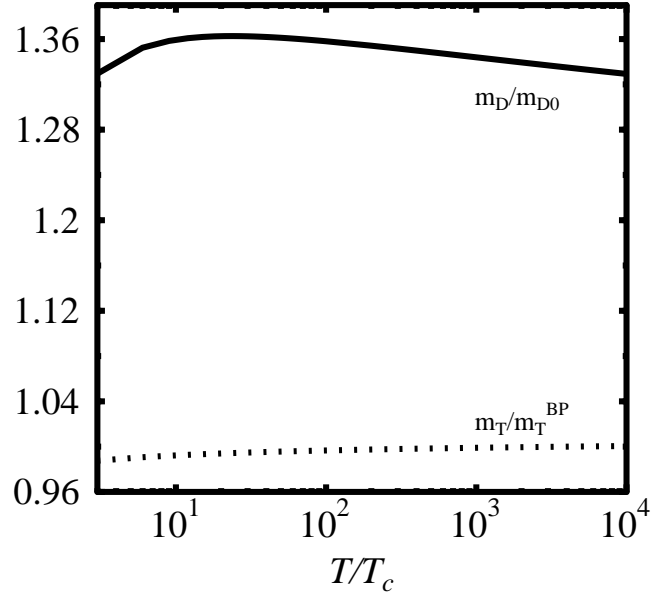


Figure 6: The temperature dependence of m_D/m_{D0} (solid line) and m_T/m_T^{BP} for Feynman ($\xi = 1$) gauge, m_{D0} is the leading order result for the Debye mass and m_T^{BP} is the value of the magnetic mass obtained by Buchmüller and Philipsen for pure $SU(2)$ gauge theory.

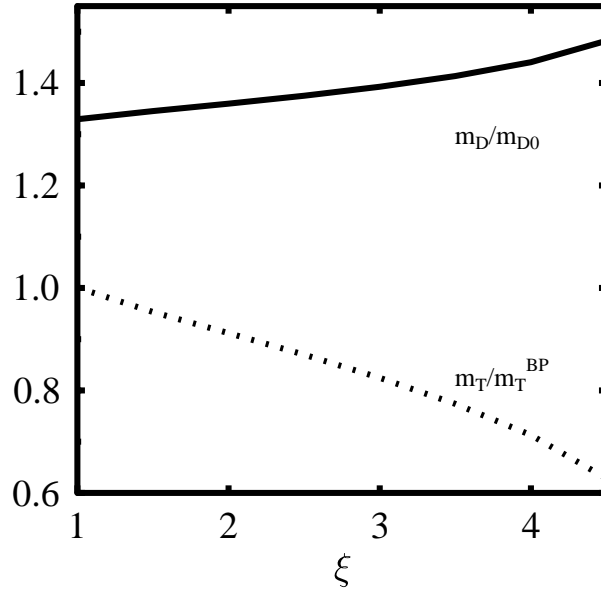


Figure 7: The dependence of m_D/m_{D0} (solid line) and m_T/m_T^{BP} on gauge parameter ξ at $T = 10^4 T_c$, m_{D0} is the leading order result for the Debye mass and m_T^{BP} is the value of the magnetic mass obtained by Buchmüller and Philipsen for pure $SU(2)$ gauge theory.

In the following numerical investigations we shall consider the case of the SU(2) gauge group. The 4-dimensional coupling constant is taken at scale $\mu = 2\pi T$, where μ is the \overline{MS} scale and 1-loop relation for the gauge parameter of the effective theory is used. To set the temperature scale we use the relation $T_c/\Lambda_{\overline{MS}} = 1.06$ obtained from numerical simulation of the finite temperature SU(2) gauge theory [49].

The temperature dependence of m_D in the Feynman gauge is plotted in Figure 6. As one can see from the plot m_D receives 30% positive correction compared to the leading order result, while the magnetic mass stays very close to the value calculated by Buchmüller and Philipsen [70], given below in Eq.(66). Since the masses are gauge dependent in this approach, it is important to investigate the dependence of the screening masses on the gauge parameter ξ . It turns out that one gets real values for the masses from the gap equations only if $\xi \in [1, 5)$. The dependence of the screening masses on ξ in this range is shown in Figure 7. One can see, that the ξ -dependence of m_T in this interval is 40 %, while for m_D it remains in the 10 % range.

3.2 Gauge Invariant Approach

Gauge invariant approaches for the magnetic mass generation in three-dimensional pure SU(N) gauge theory were suggested by Buchmüller and Philipsen (BP) [70] and by Alexanian and Nair (AN) [72]. The basic idea of both approaches is to add and subtract a gauge invariant mass generating term to the original Lagrangian:

$$L = \frac{1}{4}F_{ij}^a F_{ij}^a + \delta L - l\delta L, \quad (63)$$

where l is the (formal) loop expansion parameter. In the final result one should set $l = 1$ of course. In the scheme of BP δL is just the Lagrangian of the gauged non-linear sigma model. In the scheme of AN the mass generating term relevant for 1-loop calculation assumes the form [72]

$$\delta L = \frac{1}{2}m_T^2 A_i (\delta_{ij} - \frac{\partial_i \partial_j}{\partial^2}) A_j + f^{abc} V_{ijk} A_i^a A_j^b A_k^c, \quad (64)$$

where the explicit expression for V_{ijk} can be find in Ref. [72]. Till now only these two gauge invariant schemes are known to provide real values for the magnetic mass [73].

In these approaches the gauge boson self-energy is automatically transverse and there is no need to project the transverse part from the polarisation tensor. The corresponding expression for the on-shell self-energy reads

$$\Pi_T(k = im_T, m_T) = C m_T, \quad (65)$$

where

$$C = \begin{cases} \frac{g^2 N}{8\pi} [\frac{21}{4} \ln 3 - 1], & AN, \\ \frac{g^2 N}{8\pi} [\frac{63}{16} \ln 3 - \frac{3}{4}], & BP. \end{cases} \quad (66)$$

In gauge invariant approaches the ghost field remains massless and there is no gap equation corresponding to it.

Since we are interested in calculating the screening masses in the three-dimensional SU(N) adjoint Higgs model, $\Pi_T(k, m_T)$ should be supplemented by the corresponding contribution

coming from A_0 fields. This contribution is calculated from diagrams d) and e) of the Appendix to be

$$\delta\Pi_{ij}^{A_0}(k, m_D) = \frac{g^2 N}{4\pi} \left(-\frac{m_D}{2} + \frac{k^2 + 4m_D^2}{4k} \arctan \frac{k}{2m_D} \right) \left(\delta_{ij} - \frac{k_i k_j}{k^2} \right). \quad (67)$$

It is transverse and gauge parameter independent, it also does not depend on the specific resummation scheme applied to the magnetostatic sector. It should be also noticed that it starts to contribute to the gap equation at $\mathcal{O}(g^5)$ level in the weak coupling regime, thus preserving the magnetic mass scale to be of order $g^2 T$. This is the reason why no "hierarchy" problem arises in this case, at least for moderate g values.

The self energy of A_0 depends on the specific resummation scheme. To calculate this one has to fix a specific gauge. In Ref. [73] it was shown that it is possible to integrate out the sigma fields and the resulting Lagrangian describes massive gauge fields and has no gauge-fixing and ghost terms. Therefore to calculate the self-energy of A_0 in BP scheme one should evaluate diagrams f and g in appendix A with massive vector boson propagators. The corresponding calculation leads to

$$\begin{aligned} \Pi_{00}(k, m_D, m_T) = m_{D0}^2 + \frac{g^2 N}{4\pi} \left[-m_D - m_T + \frac{2(m_D^2 - k^2 - m_T^2/2)}{k} \arctan \frac{k}{m_T + m_D} - \right. \\ \left. \frac{(k^2 + m_D^2)}{m_T^2} \left(-m_T + \frac{k^2 + m_D^2}{k} \arctan \frac{k}{m_T + m_D} \right) \right]. \end{aligned} \quad (68)$$

This expression is different from the expression of Π_{00} calculated in the gauge non-invariant approach (see eq. (61)) but its analytic properties and on-shell value is the same as of (61). For the resummation scheme of AN it is important to find a convenient gauge fixing term which reads

$$L_{g.f.}^{AN} = \frac{1}{2} \partial_i A_i^a \left(1 - m_T^2 \frac{1}{\partial^2} \right) \partial_j A_j^a \quad (69)$$

With this gauge fixing the expression for the self-energy of A_0 coincides with (61) if it is evaluated at $\xi = 1$. The coupled set of gap equations now can be written as

$$\begin{aligned} m_T^2 &= C m_T + \delta\Pi^{A_0}(k = im_T, m_D), \\ m_D^2 &= \Pi_{00}(k = im_D, m_D, m_T). \end{aligned} \quad (70)$$

The temperature dependence of m_D obtained from this coupled set of gap equations is shown in Figure 8 for both schemes, where we have again normalized the Debye mass by the leading order result, m_{D0} . The temperature dependence of the magnetic mass is shown in Figure 9, where we have normalized m_T by the value of the magnetic mass obtained for pure three-dimensional SU(2) theory, in the BP (AN) gauge invariant calculations [70, 72]. As one can see the contribution of A_0 to the magnetic mass is between 1 and 3%. From Figures 8 and 9 it is also seen that the temperature dependence of the screening masses is very similar to the temperature dependence of the respective leading order results.

3.3 Contribution of non-Local Operators to the Gap Equation

In the previous section the gap equations were derived for an effective local superrenormalizable theory. In this case the effect of non-static modes in the 2-point function were

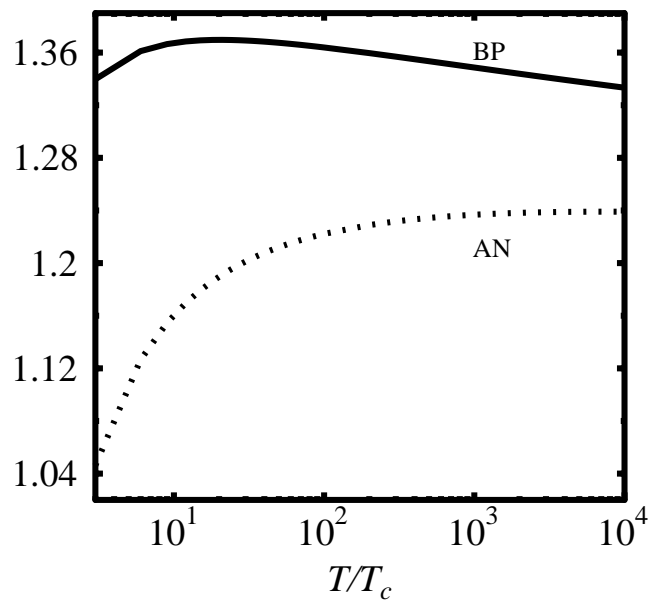


Figure 8: The temperature dependence of the scaled Debye mass for BP resummation scheme (solid) and for the AN resummation scheme (dashed). The scaling factor is m_{D0} .

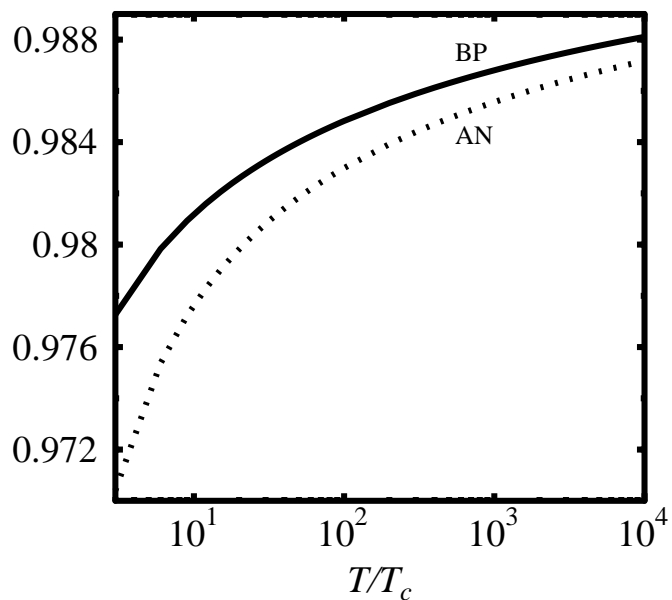


Figure 9: The temperature dependence of the scaled magnetic mass for BP resummation scheme (solid) and for the AN resummation scheme (dashed). The scaling factors are m_T^{BP} and m_T^{AN} , respectively.

represented by the thermal mass for A_0 and by the field renormalization factors which relate 3d fields to the corresponding 4d ones. It was shown in [11, 77] that when one performs the procedure of the dimensional reduction in R_ξ gauges the parameters of the superrenormalizable effective theory are gauge independent, only the expressions of 3d fields in terms of 4d ones depend on the gauge parameter. However, this does not hold for higher dimensional and non-local operators, which are generally gauge dependent. At 1-loop level the only diagrams contributing non-locally to the gap equation are those which have two non-static line inside the loop, diagrams with one static and one non-static line inside the loop are forbidden because of 4-momentum conservation. Therefore at 1-loop level the non-locality scale $(2\pi T)^{-1}$ is much smaller than the relevant length scales.

In general the non-static contribution to the static 2-point function $\Pi_{\mu\nu}(k_0 = 0, k)$ can be written as

$$\begin{aligned}\Delta\Pi_{\mu\nu}^{ns}(k_0 = 0, k) &= \delta_\mu^0\delta_\nu^0\Pi_{00}^{ns}(k) + \delta_\mu^i\delta_\nu^j(\delta_{ij} - \frac{k_i k_j}{k^2})\Pi(k), \\ \Pi_{00}^{ns}(k) &= m_{D0}^2 + a_1(\mu, \xi)k^2 + T^2 \sum_{n=2}^{\infty} a_n(\xi) \left(\frac{k^2}{2\pi T}\right)^{2n}, \\ \Pi^{ns}(k) &= b_1(\mu, \xi)k^2 + T^2 \sum_{n=2}^{\infty} b_n(\xi) \left(\frac{k^2}{2\pi T}\right)^{2n},\end{aligned}\tag{71}$$

where the coefficients a_n and b_n can be calculated for arbitrary n . The first two terms in the expressions of Π_{00} and first term of $\Pi(k)$ are already included into the 3d effective theory as part of the tree level mass and the definition of the 3d fields in term of 4d fields. The last two sums will contribute to the 3d effective lagrangian as quadratic non-local operators. There are also higher dimensional operators as well as non-local 3- and 4-point vertices in the effective lagrangian, however, since we restrict our interest to 1-loop gap equations these are not important for us. Their contribution would correspond to 2 or higher loop contribution in the full four-dimensional theory.

We have estimated by direct numerical evaluation of the infinite sums in (71) the contribution of non-local operators to be less than 1% in the temperature range $T = (3 - 10^4) T_c$, thus neither their contribution nor their gauge dependence is essential.

3.4 What Have We Learnt from the Coupled Gap Equations ?

In this section an attempt have been made to extract the electric and magnetic screening masses from the coupled set of gap equations of the three-dimensional SU(N) adjoint Higgs model considered as an effective theory of QCD. The screening masses have been studied using gauge non-invariant as well as gauge invariant resummation schemes. In the gauge non-invariant formalism we have observed rather strong gauge parameter dependence, therefore the results extracted from it are not very informative. It is still interesting to note that in Feynman gauge ($\xi = 1$) the results for the magnetic mass are rather close to those obtained from the gauge invariant resummation scheme of Buchmüller and Philipsen. In gauge invariant treatments we have compared two different resummation schemes, that of Buchmüller and Philipsen (BP) and one proposed by Alexanian and Nair (AN). Qualitatively these two resummations lead to similar results, but in the BP scheme one has smaller magnetic mass and larger Debye mass than in the AN scheme.

Let us summarize our view on the interaction of the electric A_0 and the magnetic A_i fields. In both schemes one can see that the dynamics of A_0 is largely influenced by the magnetic

sector, however, no similar feedback on the magnetic sector is seen. The magnetic masses calculated from the coupled gap equations provide screening masses which are 1% smaller than evaluated in the pure gauge theory. This fact suggests that the influence of the adjoint scalar field is similar to that of the fundamental Higgs field, because the magnetic mass calculated in the symmetric phase of 3d SU(2) Higgs theory by the gap equation technique is roughly the same as in pure gauge theory [70].

Finally we compare our results with recent Monte-Carlo data for the screening masses obtained in 4d finite temperature SU(2) gauge theory [49]. The data on the magnetic mass found from this simulation in the temperature range $T = (10 - 10^4)T_c$ can be fitted well by the formula $m_T = 0.456(6)g^2T$. This value of the magnetic mass is considerably larger than what one obtains from the magnetic gap equation and 3d simulations, where the results are approximately $m_T = 0.28g^2T$ for the BP scheme, $0.38g^2T$ for the AN scheme and $0.35(1)g^2T$ from 3d simulations. The corresponding results for the 3d adjoint Higgs model are also close to these values.

The data from Monte-Carlo simulation for the Debye mass in the above mentioned temperature interval can be fitted using the following leading order-like ansatz $\sqrt{1.69(2)}g(T)T$ [49], which means that the Debye mass is roughly $1.6m_{D0}$, where m_{D0} is the leading order result. The gap equations at the same time, as one can see from Figure 8 give $(1.2 - 1.3)m_{D0}$, depending on the resummation scheme. While there is no quantitative agreement between masses measured in Monte-Carlo simulation and those obtained from the gap equation, the temperature dependence of these masses in the temperature interval $T = (10 - 10^4)T_c$ seems to follow the temperature dependence of the leading order result.

Finally let us discuss the consistency of the gap equation approach. The validity of 1-loop gap equation for the magnetic mass in pure gauge theory was critically questioned in Refs. [78, 79]. We have seen that the two different resummation schemes lead to somewhat different results. If the gap equation approach is valid the difference between the values of the magnetic masses calculated in two schemes $m_T^{AN} - m_T^{BP}$ should be of the same order in magnitude as the 2-loop correction to the magnetic mass [73]. A recent 2-loop analysis of the magnetic mass yields $m_T = 0.34g_3^2$ [80]. Thus the gap equation approach seems to be viable. Moreover in Ref. [81] a strong coupling expansion for the magnetic mass was carried out with the result $0.32g_3^2$. In next section we will discuss the determination of the magnetic mass using lattice Monte-Carlo technique.

4 Screening Masses of Hot SU(2) Gauge Theory from Monte-Carlo Simulation of the Lattice 3d Adjoint Higgs Model

Since screening masses are static quantities it is expected that they can be determined in a 3d effective theory, the 3d SU(N) adjoint Higgs model, provided the temperature is high enough. However, in the case of the hot SU(N) gauge theory one may worry whether the standard arguments of dimensional reduction apply. First of all the coupling constant is large $g \sim 1$ for the physically interesting temperature range and thus the requirement $gT \ll \pi T$ is not really satisfied. Another problem is the identification of the physical phase of the 3d adjoint Higgs model, i.e. the phase which corresponds to the high temperature phase of SU(N) gauge theory⁸. The 3d adjoint Higgs model is known to have two phases, the symmetric (confinement) phase and the broken (Higgs) phase [82, 83, 34] separated by a line of strong 1st order transition for small Higgs couplings. The perturbative calculation of the effective potential [34, 84] suggests that the Higgs phase of the reduced theory corresponds to the deconfined phase of the 4d SU(N) theory. This conclusion seems to be supported by the 2-loop level dimensional reduction and the analysis of the phase diagram performed in Ref. [34]. Though an earlier study [28] indicated that the symmetric phase of the 3d adjoint Higgs model is the physical one, a more careful analysis shows that this conclusion may be altered by higher order corrections generated in the process of dimensional reduction (see appendix B.1). The fact that the broken phase turns out to be the physical one is contrary to naive expectations (see the discussion in the previous section). This circumstance and the $\mathcal{O}(1)$ value of the gauge coupling raises serious doubts about the validity of the dimensional reduction. Therefore a non-perturbative study is needed to clarify the applicability of the 3d effective theory.

The aim of this section is to clarify whether the screening masses, defined as poles of the corresponding lattice propagators can be determined in the effective theory for the simplest case of the SU(2) pure gauge theory. For this model precise 4d data on screening masses exist for a huge temperature range [49]. Inclusion of fermions into the model is straightforward⁹ and generalization to the SU(3) case will not introduce any novel feature.

Gauge invariant definitions of the Debye mass as it was discussed in section 2 rely on the 3d effective theory [29, 30, 34]. Although these definitions are the best in the sense that they are explicitly gauge invariant, little is known about the corresponding correlators in the full 4d theory. Gauge invariant correlators yield larger masses than the pole masses [30, 34] and further studies are required to establish the connection between them. We will try to relate these masses in section 4.5 of the thesis in the spirit of the so-called additive model [18].

⁸In the vicinity of the deconfinement phase transition the gauge coupling is very large and the dimensional reduction is certainly not valid. Therefore the two phases of the 3d adjoint Higgs model has nothing to do with the phases of 4d SU(N) gauge theory

⁹Fermionic fields do not appear in the effective theory, their role is only to modify the parameters of the effective theory.

4.1 The 3d SU(2) Adjoint Higgs Model on Lattice

The lattice action for the 3d adjoint Higgs model used in the present paper has the form

$$S = \beta \sum_P \frac{1}{2} \text{Tr} U_P + \beta \sum_{\mathbf{x}, \hat{i}} \frac{1}{2} \tilde{A}_0(\mathbf{x}) U_i(\mathbf{x}) \tilde{A}_0(\mathbf{x} + \hat{i}) U_i^\dagger(\mathbf{x}) + \sum_{\mathbf{x}} \left[-\beta \left(3 + \frac{1}{2} h \right) \frac{1}{2} \text{Tr} \tilde{A}_0^2(\mathbf{x}) + \beta x \left(\frac{1}{2} \text{Tr} \tilde{A}_0^2(\mathbf{x}) \right)^2 \right], \quad (72)$$

where U_P is the plaquette, U_i are the usual link variables and the adjoint Higgs field is parameterized, as in [34] by anti-hermitian matrices $\tilde{A}_0 = i \sum_a \sigma^a A_0^a$ (σ^a are the usual Pauli matrices). Furthermore β is the lattice gauge coupling, x parameterizes the quartic self coupling of the Higgs field and h denotes the bare Higgs mass squared. The details of the derivation of the lattice action can be found in appendix B.1.

In principle the parameters appearing in eq. (72) can be related to the parameters of the original 4d theory via the procedure of dimensional reduction [34] which is essentially perturbative and discussed in appendix B.1. The obvious problem with this approach, as it was already discussed before, is that the physical phase turns out to be the broken phase. This problem may signal that higher dimensional and non-local operators have to be kept in the effective action to ensure the consistency of the whole approach¹⁰. Certainly it is difficult to take into account all possible (higher dimensional and non-local) operators in a lattice investigation.

There are two ways out from this unfortunate situation. One can assume that the complicated action containing all kinds of higher dimensional and/or non-local operators can be mapped onto the effective action (72) which is the action of some coarse-grained theory with some finite UV cutoff and does not necessarily correspond to the naive continuum 3d adjoint Higgs model. Then parameters appearing in (72) are found by matching some quantities which are equally well calculable both in the full 4d lattice theory and in the effective 3d lattice theory, i.e. by a *non-perturbative matching*.

Another possibility which was suggested in Ref. [34] is based on observation that the parameters of the 3d adjoint Higgs model which correspond to the high temperature SU(2) gauge theory lie in the region of the parameter space which is close to the transition line and where for any finite volume available in numerical simulations the symmetric phase turns out to be metastable (see appendix B.1 for a detailed discussion on this issue). For practical purposes, e.g. measurements, the metastable phase behaves as if it was stable and thus parameters appearing in (72) can be fixed at their values given by standard dimensional reduction. One proceeds further by arguing that if higher dimensional and/or non-local operators were taken into account the transition line would be shifted so that the parameters corresponding to 4d physics would move to the region where the symmetric phase is absolutely stable but, the inclusion of these operators would have little impact on the values of the quantities we are interested in.

Here we will consider both possibilities. Comparison between corresponding 3d and 4d data, hopefully enables us to clarify which scenario takes place.

¹⁰An attempt to calculate the higher dimensional operators in the effective 3d action was recently done in Ref. [85].

Let us start to discuss the first strategy for fixing the parameters β , h , x , namely the non-perturbative matching. We will turn to the discussion of the second strategy in the next subsection. The deconfined high temperature phase of the 4d SU(2) gauge theory corresponds to some surface in the parameter space (β, h, x) , the *surface of 4d physics*. For fixed value of β the 4d physics is described by a line on this surface, which will be referred to as the *line of 4d physics*. One of the aim of numerical simulations is the determination of the surface of 4d physics. In general this would require a matching analysis in a 3d parameter space (β, x, h) , which is clearly a difficult task. We thus will follow a more moderate approach and fix two of the three parameters namely β and x , to the values obtained from the perturbative procedure of dimensional reduction. The values of these parameters at 2-loop level are [34]

$$\beta = \frac{4}{g_3^2 a},$$

$$g_3^2 = g^2(\mu) T \left[1 + \frac{g^2(\mu)}{16\pi^2} \left(L + \frac{2}{3} \right) \right], \quad (73)$$

$$x = \frac{g^2(\mu)}{3\pi^2} \left[1 + \frac{g^2(\mu)}{16\pi^2} (L + 4) \right], \quad (74)$$

$$L = \frac{44}{3} \ln \frac{\mu}{7.0555T}, \quad (75)$$

with a and T denoting the lattice spacing and temperature, respectively. The coupling constant of the 4d theory $g^2(\mu)$ is defined through the 2-loop formula

$$g^{-2}(\mu) = \frac{11}{12\pi^2} \ln \frac{\mu}{\Lambda_{\overline{MS}}} + \frac{17}{44\pi^2} \ln \left[2 \ln \frac{\mu}{\Lambda_{\overline{MS}}} \right]. \quad (76)$$

The parameter h will be left free to allow non-perturbative matching. In order to be able to compare the results of the 3d simulation with the corresponding calculations in the 4d theory it is necessary to fix the renormalization and the temperature scale. We choose the renormalization scale to be $\mu = 2\pi T$, which ensures that corrections to the leading order results for the parameters g_3^2 and x of the effective theory are small. Furthermore we use the relation $T_c = 1.06\Lambda_{\overline{MS}}$ from [49]. Now the temperature scale is fixed completely and the physical temperature may be varied by varying the parameter x . The lattice spacing was chosen according to the criterium $a \ll m^{-1} \ll Na$, where N is the extension of the lattice and m is the mass we want to measure.

4.2 Determination of the Propagators and the Screening Masses on Lattice

The main goal of this section is to study the propagators of scalar and vector (gauge) fields. For this purpose one has to fix a specific gauge, which is chosen to be the Landau gauge $\partial_\mu A_\mu = 0$. The choice of this gauge is motivated by the fact that the 4d Landau gauge

condition used in [48, 49] for static field configuration is equivalent to the 3d Landau gauge condition. On the lattice this condition is realized by maximizing the quantity [86]:

$$\text{Tr} \left[\sum_{\mathbf{x}, i} \left(U_i(\mathbf{x}) + U_i^\dagger(\mathbf{x}) \right) \right] \quad (77)$$

The gauge fixing is performed using the overrelaxation algorithm [87], which in our case is as efficient as the combined overrelaxation and *FFT* algorithm used in [48, 49]. The vector field is defined in terms of the link variables as

$$\tilde{A}_i(\mathbf{x}) = \frac{1}{2i} (U_i(\mathbf{x}) - U_i^\dagger(\mathbf{x})) \quad (78)$$

We are interested in extracting the electric (Debye) m_D and the magnetic m_T screening masses from the long distance behaviour of the scalar and vector propagators defined as

$$G_D(z) = \langle \text{Tr} \tilde{A}_0(z) \tilde{A}_0^\dagger(0) \rangle \sim \exp(-m_D z), \quad (79)$$

$$G_T(z) = \frac{1}{2} (G_1(z) + G_2(z)) \sim \exp(-m_T z), \quad (80)$$

with

$$\begin{aligned} G_i(z) &= \langle \text{Tr} \tilde{A}_i(z) \tilde{A}_i(0) \rangle, \\ \tilde{A}_\mu(z) &= \sum_{x,y} \tilde{A}_\mu(x, y, z), \quad \mu = 0, 1, 2 \end{aligned} \quad (81)$$

Note that due to the Landau gauge condition $G_3(z)$ should be constant. This fact can be used to test the precision and validity of the gauge fixing procedure. In our case this condition is satisfied with an accuracy of 0.001%.

Besides the scalar and vector propagators of the adjoint Higgs model we also calculate the gauge invariant scalar correlators and analyze the propagators also in the limit of a 3d pure gauge theory.

To extract the masses from the correlation functions we have used the general fitting ansatz

$$A \left[\frac{\exp(-mz)}{z^b} + \frac{\exp(-m(N_z - z))}{(N_z - z)^b} \right]. \quad (82)$$

Previous investigations of gauge boson and quark propagators in Landau gauge [48, 88, 89] have shown that effective masses extracted from the correlation functions rise with increasing Euclidean time separation and eventually reach a plateau. This is contrary to local masses extracted from gauge invariant correlation functions which approach a plateau from above and is a direct consequence of a non-positive definite transfer matrix in Landau gauge. A fit with $b \neq 0$ allows to extract stable masses already at shorter distances. Most of our numerical studies have been performed on lattices of size $32^2 \times 64$ ¹¹. From previous studies of gluon

¹¹ Additional calculations also have been performed on a $16^2 \times 32$ lattice and it have been checked explicitly that results for the electric mass show no volume dependence. Furthermore some calculations have been performed on a $32^2 \times 96$ lattice to check that the lattice size used for our calculations was sufficient for the determination of the magnetic mass.

propagators in the 4-dimensional SU(2) gauge theory we know that such large lattices are needed to observe a plateau in local masses [49]. In particular, this is the case for the rather small magnetic screening mass which leads to a rather slow decay of the correlation functions. We thus use the same spatial lattice size as in those studies.

We have used correlated (Michael-McKerrell) fits with eigenvalue smearing [90]. Our fits have been constrained to the region where local masses ¹² show a plateau (typically $z \sim 15$ for the magnetic mass and $z \sim 5$ for the electric mass). In this region fits with $b = 0$ and $b \neq 0$ yield mutually consistent results within statistical errors. From fits with $b \neq 0$ we find best fits with $b < 0$, in accordance with the behaviour of local masses discussed above. Although these good quality fits with $b < 0$ start at shorter distances, the magnitude of b is not well determined within our present statistical accuracy. In the following we thus will quote results from fits with $b = 0$.

4.3 Numerical Results for the Propagators of the 3d SU(2) Higgs Model

One of the aim of the numerical simulations is to clarify how far the screening mass can be determined in the framework of the effective 3d theory and to find the most suitable choice of $h(x, \beta)$.

As it was already noticed before it is expected that the symmetric phase of the 3d model corresponds to the physics of the high temperature 4d SU(2) theory. Nevertheless let us investigate the propagators in the broken phase by fixing the parameter h to its value given by perturbative dimensional reduction $h_{4d}^p(x)$. In the broken phase the simulations were done for two sets of parameters: $\beta = 16$, $x = 0.03$, $h = -0.2181$ and $\beta = 8$, $x = 0.09$, $h = -0.5159$. The propagators obtained by us in the broken phase show a behaviour which is very different from that in the symmetric phase and that in the 4d case studied in Refs. [48, 49]. The magnetic mass extracted from the gauge field propagators is $0.104(20)g_3^2$ for the first set of parameters and $0.094(8)g_3^2$ for the second set of parameters. It thus is a factor 4 to 5 smaller than the corresponding 4d result. Moreover, the propagator of the A_0 field does not seem to show a simple exponential behaviour, this fact actually is in qualitative agreement with the results of analytic calculations of Ref. [43]. Taken together these facts suggest that the broken phase does not correspond to the high T physics of the 4d system.

Now let us discuss the procedure of choosing the parameter h in the symmetric phase. The first step of this procedure is to chose for each value of x a number of trial values for h for some fixed β and measuring the propagators for these parameters. The value of β was chosen to be $\beta = 16$. The second step might be an extrapolation of the screening masses measured for different values of h for each x to the value of the screening masses obtained in 4d simulation and determination of the corresponding value of h . The guiding principle in choosing the trial values of h was the fact that these values should be close to the value corresponding to the transition. This is based on observation that the perturbative line of 4d physics lies close to the transition line. We suspect the same is true for the physically relevant h values with the exception that they are located in the symmetric phase. Therefore

¹²The definition of the local masses are given in Appendix B.2 where also futher details about the fitting procedure can be found

first we have to determine the transition line $h_c(x)$. The transition line as function of x in the infinite volume limit was found in [34] in terms of the renormalized mass parameter y (see appendix B.1 for definition of y). The transition line in terms of y turns out to be independent of β . Then using Eqs. (B.39) and (B.38) one can calculate $h_c(x)$. The usage of the infinite volume result for the transition line seems to be justified because most of our simulation were done on a $32^2 \times 64$ lattice. The two sets of $h(x)$ values, which appear on Figure 10, were chosen so that the renormalized mass parameter y always stays 10% and 25% away from the transition line. The values of the parameters in the symmetric phase are shown in Table 1 where the two sets of h values are denoted as (I) and (II) and also the values of h_c corresponding to the transition line are given. These trial values together with perturbative line of 4d physics are also depicted in Figure 10. To check the suitability of trial values shown in Table 1 simulation for $x = 0.07$ and value of $h = -0.2179$ which lies deeply in the symmetric phase was done. The corresponding value of the Debye mass was found to be $2.41(11)$. This value should be compared with the value of the Debye mass obtained $m_D/T = 1.85$ obtained in 4d case [49] for $T/T_c = 12.57$ which corresponds to $x = 0.07$. Clearly this choice of h is not suitable and one has to choose smaller h values to reproduce 4d data. The analysis described above motivated our choice of trial values for h at other values of x as given in Table 1.

<i>Temperature scale</i>		<i>h</i>		
<i>x</i>	<i>T/T_c</i>	<i>I</i>	<i>II</i>	<i>transition</i>
0.09	4.433	- 0.2652	- 0.2622	- 0.2672(4)
0.07	12.57	- 0.2528	- 0.2490	- 0.2553(5)
0.05	86.36	- 0.2365	- 0.2314	- 0.2399(6)
0.03	8761	- 0.2085	- 0.2006	- 0.2138(9)

Table 1: The two sets of the bare mass squared used in the simulation and those which correspond to the transition line for $\beta = 16$

Yet another possibility to be discussed is the simulation in the metastable symmetric phase along the line of perturbative 4d physics. As was already pointed out due to the fact that the transition line is strongly first order for all physically relevant values of x metastable symmetric branch exists below the transition line (see Figure 10). In fact the perturbative line of 4d physics lies in the region where this metastable branch exists. If one prepares the system to be in this metastable phase by starting a Monte-Carlo simulation with disordered random configuration it will not tunnel to the other broken phase corresponding to the broken phase¹³. Simulations in the metastable phase were done for parameters shown in Table 1. The temperature dependence of the screening masses obtained in the symmetric phase for two sets of the parameters, as well for the perturbative line of 4d physics $h_{4d}^p(x)$. in the metastable phase is shown in Figure 11. Also given there is the result of the 4d simulations [49], $m_D^2/T^2 = Ag^2(T)$, with $A = 1.70(2)$ for the electric mass and $m_T/T = Cg^2(T)$, with $C = 0.456(6)$ for the magnetic mass. As one can from Figure 11 the magnetic mass agrees quite well with the 4d data for both sets of h values given in Table 1 and it is not sensitive to

¹³ The tunneling between two branches is suppressed by a factor which is the exponential of the volume for all standard Monte-Carlo updating algorithms.

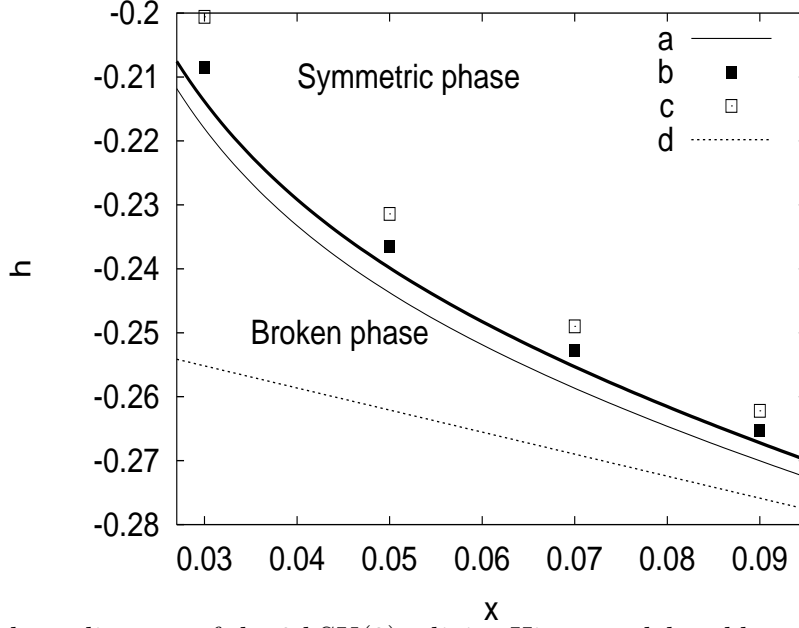


Figure 10: The phase diagram of the 3d SU(2) adjoint Higgs model and bare mass parameters h used in our analysis (squares) for $\beta = 16$: perturbative line (a) and two sets I (b) and II (c). For a discussion of their choice see text. The thick solid line is the transition line. The dashed line (d) indicates the values of h below which no metastable branch exists and was estimated based on results of Ref. [34].

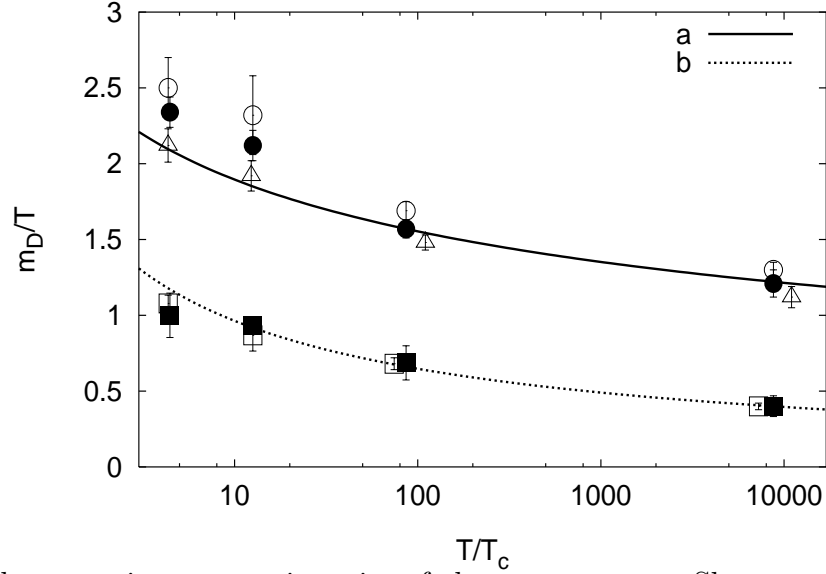


Figure 11: The screening masses in units of the temperature. Shown are the Debye mass m_D for the first (filled circles) and the second (open circles) set of h , and the magnetic mass m_T for the first (filled squares) and the second (open squares) set of h . Also shown there are the values of the Debye mass measured in metastable phase along the perturbative line of 4d physics (open triangles). The line (a) and line (b) represent the fit for the temperature dependence of the Debye and the magnetic mass from 4d simulations from [49]. Some data points at the temperature $T \sim 90T_c$ and $\sim 9000T_c$ have been shifted in the temperature scale for better visualization.

the actual value of h . The magnetic mass calculated for the perturbative line of 4d physics yields roughly the same result. The electric mass shows more pronounced dependence on h for temperatures smaller than $15T_c$ and as one can see from Figure 11 only the values of the electric mass calculated for h_{4d}^p are consistent with the 4d data. For larger temperatures the dependence of the electric mass on the actual value of h weakens but the second set of h values, which lies more deeply in the symmetric phase, seems to overestimate the value of m_D .

Based on these observations we can conclude: the the interpolation procedure for finding the true value of $h_{4d}(x)$ is not necessary and one can assume that the correct choice is $h_{4d}^p(x)$. This choice for the line of 4d physics reproduces the screening masses with about 5% accuracy in the entire temperature range. This is exactly the precision which is reasonable to assume for the 3d effective theory. Nevertheless it is important to notice that an acceptable description of the screening masses can be also achieved with the choice of h corresponding to the symmetric phase.

4.4 Magnetic Mass in 3d SU(2) Pure Gauge Theory

The magnetic mass found in the previous section seems to scale with the 3d gauge coupling $g_3^2 \sim g^2(T)T$. A similar behaviour was found for the square root of the spatial string tension in the deconfined phase of the finite temperature SU(2) gauge theory [91]. Moreover, the value of the spatial string tension is $\sqrt{\sigma_s} = 0.369(14)g^2(T)T$, which is very close to the value of the string tension calculated in the 3d pure SU(2) gauge theory: $\sqrt{\sigma_3} = 0.3340(25)g_3^2$ [92]. This behaviour can be understood for very high temperature (small coupling) because in this case, as it was discussed in subsection 2.3, the heavy A_0 field with mass $\sim gT$ can also be integrated out and the *IR* behaviour of high temperature $SU(N)$ gauge theory is described by a 3d pure gauge theory in which the only dimensionfull scale is $g_3^2 \sim g^2T$. Unfortunately for the realistic temperature range (which is also studied here) the above argument fail to hold because the coupling is large. A non-perturbative study is therefore needed to establish the relation between the magnetic mass found in the finite temperature SU(2) theory and the magnetic mass of the 3d pure gauge theory.

We have measured the Landau gauge propagators for the 3d SU(2) gauge theory and from its large distance behaviour extracted the magnetic mass. The results for different values of β are listed in Table 2.

β	m_T/g_3^2	$\chi^2/d.o.f$
12.00	0.48 ± 0.036	0.580
16.00	0.42 ± 0.070	0.497
20.00	0.44 ± 0.068	1.439

Table 2: The results of the fit for the magnetic mass in 3d pure gauge theory. Simulations for $\beta = 20$ were done on $40^2 \times 96$ lattice

Using the data from Table 2 one finds $m_T = 0.46(3)g_3^2$. This value is in good agreement with the 3d adjoint Higgs model result. The magnetic mass thus is rather insensitive to the dynamics of the A_0 field. This finding is in accordance with the gap equation study of the

adjoint Higgs model described in the previous section. Gauge boson propagators were also studied in the 3d SU(2) Higgs model in Ref. [38]. It was found that in the symmetric phase the magnetic mass extracted from the propagator is insensitive to the values of the scalar couplings and its value is $0.35(1)g_3^2$. The magnetic mass in the 3d pure gauge theory was also measured there and its value was found to a bit larger but close $0.35(1)g_3^2$ (see Figure 3 in Ref. [93]). This value is considerably smaller than the value found by us. This fact is probably due to small lattices used in Ref. [93] and to the different method for extracting the screening masses. These issues are discussed in appendix B.2.

The decoupling of static magnetic sector is also seen in study of gauge invariant correlators. In Refs. [34, 94] the mass of the lowest lying gluball was measured in the 3d SU(2) adjoint Higgs model and its value was found rather insensitive to the values of scalar couplings and close to the corresponding value of the 3d pure SU(2) gauge theory.

4.5 Gauge Invariant Correlators and the Additive Constituent Gluon Model

In this subsection I will establish a simple relation between gauge invariant and gauge dependent correlators. Gauge invariant correlators for the SU(2) adjoint Higgs model were measured in Refs. [34, 94]. The correlators of the following gauge invariant operators were studied: $\text{Tr} A_0^2$, $h_{ij} = \text{Tr} A_0 F_{ij}$ and $G = F_{ij}^a F_{ij}^a$ ¹⁴.

Let us first consider the correlation function of the scalar operator $\text{Tr} A_0^2$ whose large distance behaviour gives the mass of the $A_0 - A_0$ bound state: $m(A_0)$. The mass of this bound state is also expected to determine the exponential falloff of the Polyakov loop correlator [34]. Let us discuss the relation of $m(A_0)$ and the Debye mass defined through the propagator. If the coupling constant is small enough then $m(A_0) \sim 2m_{D0}$. In our case this perturbative relation is not satisfied. However, following the analysis of Ref. [18] the mass of the $A_0 - A_0$ bound state can be represented by the sum of two constituent adjoint scalar masses, which is m_D .

Next we discuss the gauge invariant correlator containing gauge field operators. In Ref. [18] it was suggested that the screening masses extracted from these correlators can be related to the screening masses extracted from propagators using the notion of the constituent gluon. According to this idea one can associate with each covariant derivative in the corresponding operator a constituent gluon with the mass equal to the propagator pole mass m_T . It was shown in Ref. [18] that using this simple idea the spectrum of 3d SU(2) Higgs model can be qualitatively well interpreted. The mass of the lowest lying glueball state was measured in Ref. [94]¹⁵ and was found to be rather independent of the couplings h and x of the A_0 field, the value of this mass is $m_G \sim 1.67(2)g_3^2$. In terms of the constituent model this state can be viewed as a loose bound state of four constituent gluons [18] with a constituent mass equal to m_T , thus $m_G \sim 4m_T$. If one uses the value of magnetic mass in pure gauge theory found in Monte-Carlo simulations one finds $m_G = 1.84(12)g_3^2$. For the value of the magnetic mass given by Nair [81] one gets $m_G \sim 1.28g_3^2$.

¹⁴In Ref.[34] the correlation function of the operator $h_i = \epsilon_{ijk} \text{Tr} A_0 F_{jk}$ was studied instead of h_{ij} . But the masses extracted from this correlation function are close to those extracted from h_{ij}

¹⁵Earlier measurements of Ref. [34] overestimated the mass of this state.

An attempt for a gauge invariant definition of the constituent gluon mass was given in Ref. [31]. The approach is based on the expectation value of the following operator

$$G_{Fijkl}(x, y) = \langle F_{ij}^a(x) U_{ab}(x, y) F_{kl}^b(y) \rangle, \quad (83)$$

where

$$\begin{aligned} U_{ab}(x, y) &= 2\text{Tr} T^a U(x, y) T^b U^\dagger(x, y), \\ U(x, y) &= P \exp\left(ig \int_x^y dx_i A_i^a T^a\right) \end{aligned} \quad (84)$$

with T^a being SU(N) generators. For large separation one has $G_F \sim \exp(-M_s|x - y|)$. According to the additive constituent gluon model $M_s = 2m_T$. The numerical value was found to be $M_s \sim 0.73g_3^2$. Based on the additive constituent gluon model and the numerical value of the magnetic mass in pure SU(2) gauge theory one would expect $M_s \sim 0.92(6)g_3^2$. On the other hand with the value of the magnetic mass obtained by Nair [81] one expects $M_s = 0.64g_3^2$.

Finally we consider the correlation function of h_{ij} . This correlation function was used for non-perturbative definition of the Debye mass [30, 31, 32]. In terms of the additive constituent gluon model the mass extracted from this correlation function is $m_h = m_D + 2m_T$. The masses predicted by the constituent model compared with the results of direct measurements are shown in Table 3.

<i>parameters</i>			$m(A_0)/g_3^2$		m_h/g_3^2	
β	x	h	<i>measured</i>	<i>constituent model</i>	<i>measured</i>	<i>constituent model</i>
9	0.10	-0.4764	1.01(2) ^a	1.75(18)	1.39(6) ^a	1.79(15) [1.51(1)]
16	0.09	-0.2622	1.54(15)	1.78(6)		
16	0.05	-0.2314	2.28(20)	2.38(16)		
9	0.04	-0.2883	2.41(2) ^a	2.74(2)	2.16(20) ^a	2.29(7) [2.01(1)]
32	0.04	-0.1247	2.20(11) ^b	2.42(1)	2.42(15) ^b	2.12(7) [1.85(1)]
24	0.03	-0.1475	3.03(65)	3.28(30)		

Table 3: The masses of the adjoint scalar and heavy-light bound states in units of g_3^2 compared with the predictions of the additive constituent gluon model. Some bound state masses were taken from Ref. [94] (a) and Ref. [34] (b), other values were taken from Ref. [50]. In square brackets we indicate the predictions of the constituent gluon model based the value of the magnetic mass estimated by Nair [81].

As one can see from the Table except for the largest value of x which corresponds to the temperature $T \sim 3T_c$ the simple additive model can describe the spectrum of gauge invariant screening masses with the accuracy of 15 – 20%. This is the accuracy which is reasonable to expect from such simple bound state picture which does not take into account binding energy.

The success of the additive model in describing the mass of the $A_0 - A_0$ bound state has important physical consequence concerning the physics of the screening defined from the

Polyakov loop correlator. In section 2.4 it was argued that the true large distance behaviour of the Polyakov loop correlator is determined by the lightest 3d gluball state. However, as one can see from Table 3 for $x \leq 0.5$ the masses extracted from the $\text{Tr} A_0^2$ correlator are larger than the 3d gluball mass and can be well described by the additive model. This suggests that the dominant contribution to the Polyakov loop correlator comes from the exchange of two constituent A_0 field in a similar manner as it happens in the leading order of perturbation theory.

4.6 Gauge Dependence of the Screening Masses

Before closing this section we briefly want to address the question of a possible gauge dependence of the screening masses extracted by us. The pole of the propagator was proven to be gauge invariant in perturbation theory [42, 95]. The statement on the propagator pole masses extracted from lattice simulation is less clear. Here one faces the numerical problem to isolate the asymptotic large distance behaviour of the correlation function from possible short distance (powerlike) corrections which are gauge dependent [88]. In Ref. [89] quark-propagators were studied in axial, Coulomb and Landau gauges and the effective masses extracted at quite short physical distances were found to depend on the gauge. In Ref. [88] the quark and gluon propagators were investigated in so-called λ -gauges. Masses extracted from the propagators using exponential fits like Eq. (82) also show a mild dependence on the gauge parameter. To study the gauge dependence of our results, following, [88] we have introduced λ -gauges which in our case are defined by the condition

$$\lambda \partial_3 A_3 + \partial_2 A_2 + \partial_1 A_1 = 0. \quad (85)$$

The propagators have been measured in λ gauges and the masses were extracted from the propagators using the functional form given in Eq. (82).

Some preliminary results on the gauge dependence of the screening masses were already published in [96]. However the conclusion presented there are somewhat different from the present situation due to the low statistics of the first analysis.

For the numerical analysis the following values of the parameter λ have been chosen : $\lambda = 0.5, 1.0, 2.0, 8.0$. Simulations were performed on a $32^2 \times 96$ lattice at $x = 0.03$ and for two values of β and h . Values of the Debye mass measured for different λ and two values of β are summarized in Table 4.

λ	0.5	1.0	2.0	8.0
$\beta = 16, h = -0.2085$	1.28(6)	1.21(9)	1.15(5)	1.08(6)
$\beta = 24, h = -0.1510$	1.26(7)	1.31(9)	1.20(5)	1.11(3)

Table 4: The Debye mass in units of the temperature for $x = 0.03$ and calculated for different λ parameters.

As one can see from the results the Debye mass shows a weak dependence on λ . Its value is decreasing as λ increases but for $\lambda \geq 2$ it seems to approach a constant value which is independent of λ . This dependence on λ is similar to those which was found in Ref. [88]. In Figure 12 we show the local electric masses for $\beta = 24$ and $h = -0.1510$ for the largest ($\lambda = 8$) and the smallest ($\lambda = 0.5$) values of the λ parameter.

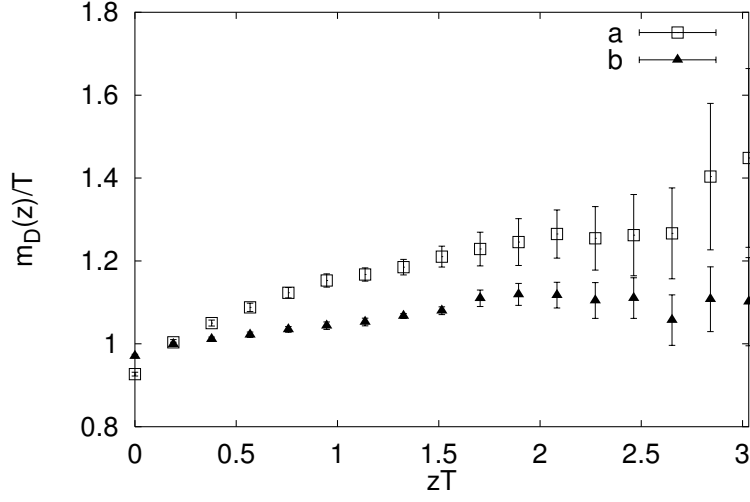


Figure 12: The local electric masses for $\beta = 16$, $x = 0.03$ and $h = -0.1510$ in units of g_3^2 measured on $32^2 \times 96$ lattice for different values of the gauge parameter λ . Shown are the local electric mass for $\lambda = 0.5$ (a) and for $\lambda = 8.0$ (b).

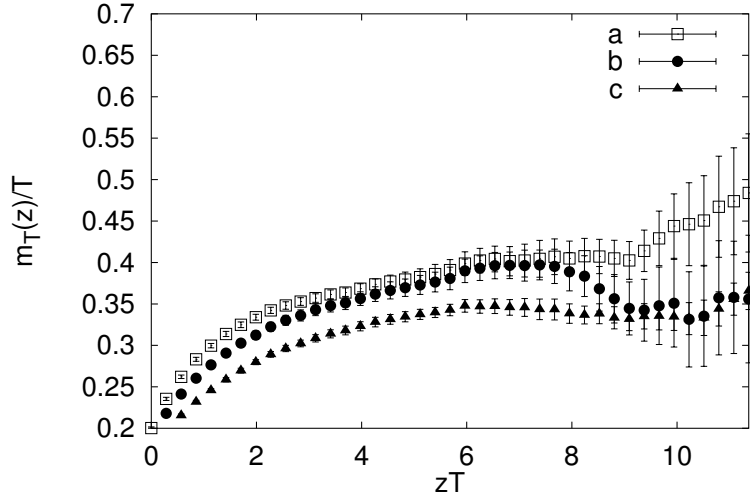


Figure 13: The local magnetic masses for $\beta = 16$, $x = 0.03$ and $y = 0.9279$ in units of g_3^2 measured on $32^2 \times 96$ lattice for different values of the gauge parameter λ . Shown are the local magnetic mass for $\lambda = 0.5$ (a), for $\lambda = 1.0$ (b) and for $\lambda = 2.0$ (c).

The local magnetic masses measured at $\beta = 16$, $x = 0.03$ and $h = -0.2085$ for $\lambda = 0.5, 1.0, 2.0$ are shown in Figure 13. Similar to the electric mass the magnetic mass also show a mild dependence on λ .

Further studies are required to clarify the source of the non-perturbative gauge dependence of the screening masses.

5 Coupled Gap Equation for SU(2) Higgs Model

As it was already mentioned in the Introduction, considerable progress has been achieved in understanding the thermodynamics of the electroweak phase transition in the past 5 years. For the electroweak theory the separation of different mass scales holds ($2\pi T \gg gT \gg g^2 T$)¹⁶ and the superheavy modes (i.e. the non-zero Matsubara modes with typical mass $\sim 2\pi T$) together with the heavy A_0 field (with a mass $\sim gT$) are integrated. The thermodynamics is described by an effective theory, the 3d SU(2) Higgs model [10, 11, 12, 40]. The properties of the phase transition and the screening masses were studied in great detail using lattice Monte-Carlo simulations of the reduced model [19, 93]. The application of the gap equation approach [68, 70] led to similar results. Both approaches predict that the line of first order transitions ends for some Higgs mass $m_H = m_H^c$ and the value of the critical mass m_H^c was found to be the same within 20%.

Recent 4d Monte-Carlo simulations of the finite temperature SU(2) Higgs model [97, 98] provide good non-perturbative tests for the validity of dimensional reduction. A detailed discussion of relating 4d and 3d results was published very recently in Ref. [99].

The purpose of the investigations presented in this section is twofold. The first aim is to provide some non-perturbative evidence for the decoupling of the A_0 field from the gauge + Higgs dynamics in the vicinity of the phase transition. The coupled set of gap equations for the screening masses will be derived and solved numerically in the 3d fundamental + adjoint Higgs model. This model emerges when the non-static modes are integrated out in the full finite temperature Higgs system. Its predictions for the screening masses will be compared with those obtained by Buchmüller and Philipsen (BP) [70] in the 3d Higgs model using the same technique. This model is obtained from the 3d fundamental + adjoint Higgs model by integrating out the heavy A_0 field. The main result of this comparison is a proposition for a non-perturbative and non-linear mapping between the two models ensuring quantitative agreement between the screening masses in a wide temperature range on both sides of the transition. This high quality evidence for the decoupling of the A_0 field at the actual finite mass ratios presumes, however, the knowledge of the "exact" value of the Debye screening mass, since for the proposed mapping its non-perturbatively determined value turns out to be essential.

The second aim of the present investigations is to examine the symmetric phase in more detail. There the Higgs and the Debye screening masses are both of the same order of magnitude $\sim gT$ and thus in that regime there is no *a priori* reason for the A_0 field to decouple. This circumstance makes the quantitative relation of the screening masses calculated in the 3d fundamental + adjoint Higgs model particularly interesting in the high-T phase. Here we are going to apply two different resummation techniques and check to what extent persists a non-perturbative mass hierarchy in this part of the spectra. Investigations presented in this Section are based on Ref. [100].

¹⁶The renormalized gauge coupling for the electroweak theory has a moderate value $g \sim 0.66$. In the following discussion we will ignore the presence of the U(1) sector and fermions because they are not essential from the point of view of basic properties of the electroweak phase transition.

5.1 The Extended Gap Equations

The Lagrangian of the three dimensional SU(2) fundamental + adjoint Higgs model is [70, 11]

$$L^{3D} = \text{Tr} \left[\frac{1}{2} F_{ij} F_{ij} + (D_i \Phi)^\dagger (D_i \Phi) + \mu^2 \Phi^\dagger \Phi + 2\lambda (\Phi^\dagger \Phi)^2 \right] \\ + \frac{1}{2} (D_i \vec{A}_0)^2 + \frac{1}{2} \mu_D^2 \vec{A}_0^2 + \frac{\lambda_A}{4} (\vec{A}_0^2)^2 + 2c \vec{A}_0^2 \text{Tr} \Phi^\dagger \Phi, \quad (86)$$

where

$$\Phi = \frac{1}{2} (\sigma 1 + i\vec{\pi}\vec{\tau}), \quad D_i \Phi = (\partial_i - igW_i)\Phi, \quad W_i = \frac{1}{2} \vec{\tau} \vec{W}_i. \quad (87)$$

The relations between the parameters of the 3d theory and those of the 4d theory are derived at 1-loop level perturbatively [11]:

$$g^2 = g_{4d}^2 T, \quad \lambda = \left(\lambda_{4d} + \frac{3}{128\pi^2} g_{4d}^4 \right) T, \quad \lambda_A = \frac{17}{48\pi^2} g_{4d}^4 T, \\ c = \frac{1}{8} g_{4d}^2 T, \quad \mu_D^2 = \frac{5}{6} g_{4d}^2 T^2, \quad \mu^2 = \left(\frac{3}{16} g_{4d}^2 + \frac{1}{2} \lambda_{4d} \right) T^2 - \frac{1}{2} \mu_{4d}^2. \quad (88)$$

If the integration over the A_0 adjoint Higgs field is performed we obtain the model investigated in [70] with parameters $\bar{g}, \bar{\lambda}, \bar{\mu}$. These couplings of the reduced theory are related to the parameters of the 3d fundamental + adjoint Higgs theory through the following relations:

$$\bar{g}^2 = g^2 \left(1 - \frac{g^2}{24\pi\mu_D} \right), \quad \bar{\lambda} = \lambda - \frac{3c^2}{2\pi\mu_D}, \quad \bar{\mu}^2 = \mu^2 - \frac{3c\mu_D}{2\pi}. \quad (89)$$

In particular, we note that the $\bar{\mu}$ scale serves as the temperature scale of the fully reduced system, while μ is the scale for the system containing both the fundamental and the adjoint scalars. The two are related perturbatively by a constant shift.

In order to perform the actual calculations in the broken phase it is necessary to shift the Higgs field, $\sigma \rightarrow v + \sigma'$. After this shift and the gauge-fixing (the gauge fixing parameter is denoted by ξ) the Lagrangian including the ghost terms assumes the form

$$L = \frac{1}{4} \vec{F}_{\mu\nu} \vec{F}_{\mu\nu} + \frac{1}{2\xi} (\partial_\mu \vec{W}_\mu)^2 + \frac{1}{2} m_{T0}^2 \vec{W}_\mu^2 \quad (90)$$

$$+ \frac{1}{2} (\partial_\mu \sigma')^2 + \frac{1}{2} M_0^2 \sigma'^2 + \frac{1}{2} (\partial_\mu \vec{\pi})^2 + \xi \frac{1}{2} m_{T0}^2 \vec{\pi}^2 \quad (91)$$

$$+ \frac{g^2}{4} v \sigma' \vec{W}_\mu^2 + \frac{g}{2} \vec{W}_\mu \cdot (\vec{\pi} \partial_\mu \sigma' - \sigma' \partial_\mu \vec{\pi}) + \frac{g}{2} (\vec{W}_\mu \times \vec{\pi}) \cdot \partial_\mu \vec{\pi} \quad (92)$$

$$+ \frac{g^2}{8} \vec{W}_\mu^2 (\sigma'^2 + \vec{\pi}^2) + \lambda v \sigma' (\sigma'^2 + \vec{\pi}^2) + \frac{\lambda}{4} (\sigma'^2 + \vec{\pi}^2)^2 \quad (93)$$

$$+ \frac{1}{2} (D_i \vec{A}_0)^2 + \frac{1}{2} m_{D0}^2 \vec{A}_0^2 + \frac{\lambda_A}{4} (\vec{A}_0^2)^2 + 2cv\sigma' \vec{A}_0^2 + c\vec{A}_0^2 (\sigma'^2 + \vec{\pi}^2)$$

$$+ \partial_\mu \vec{c}^* \partial_\mu \vec{c} + \xi m_{T0}^2 \vec{c}^* \vec{c} \quad (94)$$

$$+ g \partial_\mu \vec{c}^* \cdot (\vec{W}_\mu \times \vec{c}) + \xi \frac{g^2}{4} v \sigma' \vec{c}^* \vec{c} + \xi \frac{g^2}{4} v \vec{c}^* \cdot (\vec{\pi} \times \vec{c}) + \frac{1}{2} \mu^2 v^2 + \frac{1}{4} \lambda v^4 \quad (95)$$

$$+ \frac{1}{2} (\mu^2 + \lambda v^2) (\sigma'^2 + \vec{\pi}^2) + v (\mu^2 + \lambda v^2) \sigma' , \quad (96)$$

where the following notations were introduced for the tree-level masses: $m_{T0}^2 = \frac{1}{4} g^2 v^2$ (the vector boson mass), $M_0^2 = \mu^2 + 3\lambda v^2$ (the Higgs mass) and $m_{D0}^2 = \mu_D^2 + 2cv^2$ (the Debye mass). The last two terms of (97) arise from the Higgs potential after the shift in the Higgs field σ . For $\mu^2 < 0$, they vanish if one expands around the classical minimum $v^2 = -\mu^2/\lambda$. These terms have to be kept [70], when the equation for the vacuum expectation value is to be deduced.

In order to obtain the coupled gap equations one replaces the tree-level masses by the exact masses

$$m_{T0}^2 \rightarrow m_T^2 + \delta m_T^2, \quad M_0^2 \rightarrow M^2 + \delta M^2, \quad m_{D0}^2 \rightarrow m_D^2 + \delta m_D^2, \quad (98)$$

and treats the differences $\delta m_T^2 = m_{T0}^2 - m_T^2$, $\delta M^2 = M_0^2 - M^2$, $\delta m_D^2 = m_{D0}^2 - m_D^2$ as counterterms. The exact Goldstone and ghost masses are both equal to $\sqrt{\xi} m_T$, where m_T is the exact gauge boson mass. The gauge invariance of the self-energies of the Higgs and gauge bosons is ensured by introducing appropriate vertex resummations. Their explicit formulae can be found in [70]. In the present extended model, a resummation of the Higgs- A_0 vertex would be also necessary if the gauge invariance of the A_0 self-energy is to be ensured. Then the only source of the gauge dependence which would remain is the equation for the vacuum expectation value v .

All these resummations are equivalent to work with the following gauge invariant Lagrangian:

$$\begin{aligned} L_I^{3D} = & \frac{1}{4} \vec{F}_{ij} \vec{F}_{ij} + Tr \left((D_i \Phi)^+ D_i \Phi - \frac{1}{2} M^2 \Phi^+ \Phi \right) + \frac{1}{2} (m_D^2 - \frac{8cm_T^2}{g^2}) \vec{A}_0^2 \\ & + \frac{g^2 M^2}{4m_T^2} Tr(\Phi^+ \Phi)^2 + 2c \vec{A}_0^2 Tr \Phi^+ \Phi. \end{aligned} \quad (99)$$

In this Lagrangian one shifts the Higgs field around its classical minimum $\sigma \rightarrow \sigma' + \frac{2m_T}{g}$ and adds the corresponding gauge fixing and ghost terms [70]. Shortly, we shall argue that the A_0 -Higgs vertex resummation arising from the replacement of v by $2m_T/g$ when the scalar field is shifted in the last term of the above Lagrangian destroys the mass-hierarchy between the heavy A_0 and the light gauge and Higgs fields. Therefore we have to give up the full gauge independence of the resummation scheme. The numerical solution to be presented below shows that the gauge dependence of the $A_0 - \Phi$ vertex in our resummation scheme introduces only a minor additional gauge dependence beyond that of the equation for the vacuum expectation value [70] appearing below in Eq. (106).

The coupled set of gap equations is constructed from that of Ref. [70] by adding the contributions due to the presence of the adjoint Higgs field. The self-energy contributions for the 3d adjoint Higgs model were already calculated in section 3. Below we list only the additional contributions to the self-energies, which all contain at least one $A_0 - \Phi$ vertex (the corresponding diagrams are listed in the Appendix B). Let us emphasize once again that no resummation of the $A_0 - \Phi$ vertex was applied.

The additional contribution to the self-energy of the A_0 field coming from Higgs, Goldstone, gauge and ghost fields (diagrams **a-i**) is

$$\begin{aligned} \delta\Pi_{A_0}^{H,G,gh} = & -\frac{4cv^2(\mu^2 + \lambda v^2)}{M^2} + \frac{3cgv}{\pi} \left(\frac{M}{4m_T} + \frac{m_T^2}{M^2} \right) - \frac{cM}{2\pi} + \frac{3\sqrt{\xi}}{4\pi} (gv - 2m_T) \\ & + \frac{4c^2v^2}{\pi} \left[\frac{3}{2} \frac{m_D}{M^2} - \frac{1}{p} \arctan \frac{p}{m_D + M} \right]. \end{aligned} \quad (100)$$

There is also an additional contribution to the gauge boson self-energy coming from the adjoint Higgs field (diagram **m**):

$$\delta\Pi_T^H(p, m_T, M, m_D) = \frac{3cg}{2\pi} \frac{m_T v}{M^2} m_D. \quad (101)$$

The contribution of \vec{A}_0 to the Higgs self-energy (diagrams **j-l**) is the following:

$$\delta\Pi_H^{A_0}(p, m_T, m_D) = -\frac{3m_D c}{2\pi} - \frac{6c^2v^2}{\pi} \frac{1}{p} \arctan \frac{p}{2m_D} + \frac{9gcv}{4\pi m_T} m_D. \quad (102)$$

Making use also of the pieces of the self-energies calculated in section 3 and also in [70] we write down a set of coupled on-shell gap equations for the screening masses of the magnetic gauge bosons, fundamental Higgs and adjoint A_0 fields in the form:

$$\begin{aligned} m_T^2 = & \Pi_T(p^2 = -m_T^2, m, M) + \delta\Pi_T^{A_0}(p^2 = -m_T^2, m_D) \\ & + \delta\Pi_T^H(p^2 = -m_T^2, m_T, M, m_D) \end{aligned} \quad (103)$$

$$M^2 = \Sigma(p^2 = -M^2, m_T, M) + \delta\Pi_H^{A_0}(p^2 = -M^2, m_T, m_D), \quad (104)$$

$$m_D^2 = \Pi_{00}(p^2 = -m_D^2, m_T, m_D) + \delta\Pi_{A_0}^{H,G,gh}(p^2 = -m_D^2, m_T, M, m_D), \quad (105)$$

where Π_T and Σ are defined by Eqs. (17), (18) of Ref. [70]. $\delta\Pi_T^{A_0}$ and Π_{00} are defined by Eqs. (67) and (61).

If on the right hand side of the third equation one inserts the tree level masses, the next-to-leading order result of Ref.[101] is recovered for the Debye mass in the SU(2) Higgs model.

The equation for the vacuum expectation value completes the set of the above three equations:

$$v(\mu^2 + \lambda v^2) = \frac{3}{16\pi} g \left(4m_T^2 + \sqrt{\xi} M^2 + \frac{M^3}{m_T} \right) + \frac{3c}{2\pi} v m_D. \quad (106)$$

It is important to notice that this equation can be rewritten as

$$v(\mu_{eff}^2 + \lambda v^2) = \frac{3}{16\pi} g \left(4m_T^2 + \sqrt{\xi} M^2 + \frac{M^3}{m_T} \right), \quad (107)$$

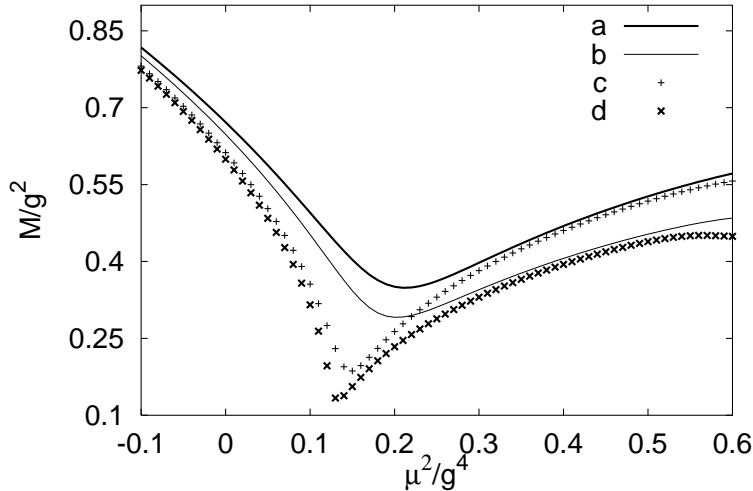


Figure 14: The Higgs mass in units of g^2 as function of μ^2/g^4 calculated at $\lambda/g^2 = 1/8$ using the gauge-invariant $A_0 - \Phi$ vertex resummation version of the gap equations. Shown are the Higgs mass derived in the full static theory in the Landau- (a) and in the Feynman-gauge (b) and the Higgs mass, and in the A_0 -reduced theory in the Landau-gauge (c) and in the Feynman-gauge (d). The μ^2 -shift indicated by eq.(89) was applied.

with

$$\mu_{eff}^2 = \mu^2 - \frac{3c}{2\pi} m_D. \quad (108)$$

This equation is formally identical to the equation of BP for the vacuum expectation value [70]. On the basis of this observation, we expect that the main effect of the A_0 integration is the above shift in the μ^2 -scale. Since m_D is itself a non-trivial function of μ this non-perturbative mapping is also nonlinear.

A very similar set of equations could be derived for the case of the gauge invariant resummation of the $A_0 - \Phi$ vertex. For instance, one would write in the last term on the right hand side of (106) $2m_T/g$ on the place of v , which would prevent the absorption of this term into a redefinition of the temperature scale. This was the reason when we solved the gap equations first for the case of gauge invariant $A_0 - \Phi$ vertex resummation, that we have found substantial corrections to the BP results, beyond the shift of the μ^2 -scale indicated in eq. (89). This situation is illustrated in Figure 14.

This makes it clear that the decoupling of the A_0 -field for the physical value of the parameter c would not work, the hierarchy of the screening masses would be destroyed under such vertex resummation scheme. Since our goal is to propose such a mapping onto the fundamental Higgs-model, which already for finite A_0 -mass shows evidence for the asymptotic Appelquist-Carazzone theorem [39], we have renounced from the gauge invariant resummation of the $A_0 - \Phi$ vertex.

5.2 Numerical Results

The main goal of the present investigation is to analyze non-perturbatively in quantitative terms the decoupling of the A_0 field. We are interested in those effects which go beyond the

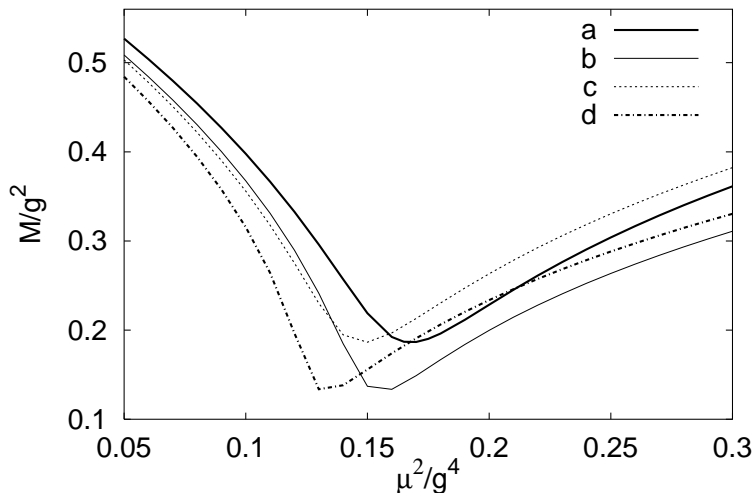


Figure 15: The Higgs boson masses at $\lambda/g^2 = 1/8$ (crossover region) in units of g^2 as function of μ^2/g^4 in the 3d fundamental + adjoint Higgs model and in the 3d SU(2) Higgs (A_0 -reduced) theory. Shown are the Higgs mass in the full static theory in the $\xi = 0$ (Landau) gauge (a) and in the $\xi = 1$ (Feynman) gauge (b), and the Higgs boson mass in the A_0 -reduced theory in the $\xi = 0$ gauge (c) and in the the $\xi = 1$ gauge (d).

perturbative mapping implied by eq.(89). Therefore, we will first compare the predictions for the Higgs and gauge boson masses from the coupled gap equations (103)-(106) of the 3d fundamental + adjoint Higgs model with those obtained in the A_0 -reduced theory, the 3d Higgs model [70]. The corresponding Higgs masses are shown in Figure 15 using two different gauges. The results obtained in the A_0 -reduced theory are displayed after the shift required by eq.(89) is performed. The difference between the full and the reduced theory is still visible in the vicinity of the crossover. In this region the relative difference between the prediction of the full and the reduced theory is about 20%.

Our proposal to resolve this relatively large deviation is to introduce a more complicated relationship between the couplings. Having gained intuition from eq.(108), we have plotted the mass-predictions for the Higgs-field derived from our full set of equations against the results of BP calculated for couplings taken from (89) with a replacement $\mu_D \rightarrow m_D$:

$$g_{eff}^2 = g^2 \left(1 - \frac{g^2}{24\pi m_D}\right), \quad \lambda_{eff} = \lambda - \frac{3c^2}{2\pi m_D}, \quad \mu_{eff}^2 = \mu^2 - \frac{3c}{2\pi} m_D. \quad (109)$$

The non-trivial nature of this replacement becomes clear from Figure 16 where the μ^2 -dependence of m_D is displayed. Clearly, its non-trivial μ^2 -dependence is most expressed in the neighbourhood of the phase transformation (crossover) point $\mu^2/g^4 \in (0.1 - 0.2)$. The application of this mapping to the data obtained from the model containing both the fundamental and the adjoint representation leads to a perfect agreement of the two data sets for large values of λ/g^2 . For smaller values of λ/g^2 (1/32, 1/64) the mapping (109) works very well in the symmetric phase, but in the broken phase (89) seems to be the better choice.

We suspect, that the tree level piece in m_D arising from the Higgs-effect, should not be included into the correction of (89), since it is itself a tree-level effect. Therefore we propose

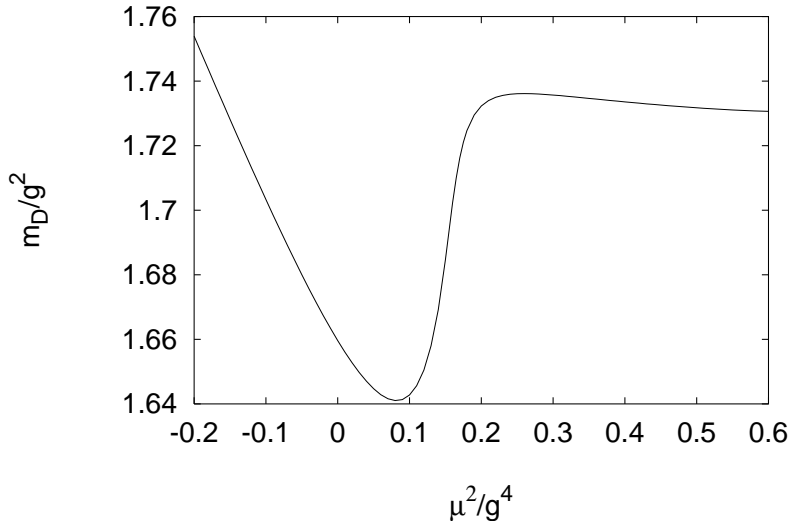


Figure 16: The μ^2 dependence of the Debye mass for $\frac{\lambda}{g^2} = 1/8$.

the following replacement in (109):

$$m_D \rightarrow \sqrt{m_D^2 - 2cv^2}. \quad (110)$$

In Figure 17 it is obvious that a very good agreement could be obtained with this mapping between the Higgs mass predictions of the one-loop gap equations of the full static and the A_0 -reduced theory for $\lambda/g^2 = 1/32$. The quality of the agreement on both sides of the phase transition is good, signalling that the influence of the “mini-Higgs” effect in the symmetric phase is negligible. Therefore it is not surprising that for $\lambda/g^2 = 1/8$ the same quality of agreement is obtained like before.

It is important to notice that there is a strong gauge parameter dependence in the symmetric phase and in the vicinity of the crossover. The variations due to the change in the gauge are equal in the full and in the reduced theory, which indicates that the additional gauge dependence, introduced by the gauge non-invariant resummation of the A_0 field is negligible. The mapping (110) performs equally well in Landau- and Feynman-gauges.

Other quantities which are worth of considering for the comparison of the full 3d and the reduced theories are λ_c/g^2 , the endpoint of the first order transition line and μ_+/g^2 , the mass parameter above which the broken phase is no longer metastable. The values of μ_+^2/g^4 for different scalar couplings and different gauges in the full and in the reduced theory are summarized in Table 1. Here the mapping (109) could be implemented only by extrapolating from smaller μ^2/g^4 , since the end-points of metastability do not correspond to each other, and in some cases m_D could not be determined from the gap equations. Also here for larger values of λ/g^2 the application of (109) led to an improved agreement between the end-point μ_+^2/g^4 values, while for $\lambda/g^2 = 1/48, 1/64$ the mapping (89) works better. In the table we have displayed μ_+^2/g^4 values of the A_0 -reduced theory shifted perturbatively and with help of the best performing non-perturbative mapping (110). For both gauges the latter agrees with the μ_+^2/g^4 -values of the full static theory very well.

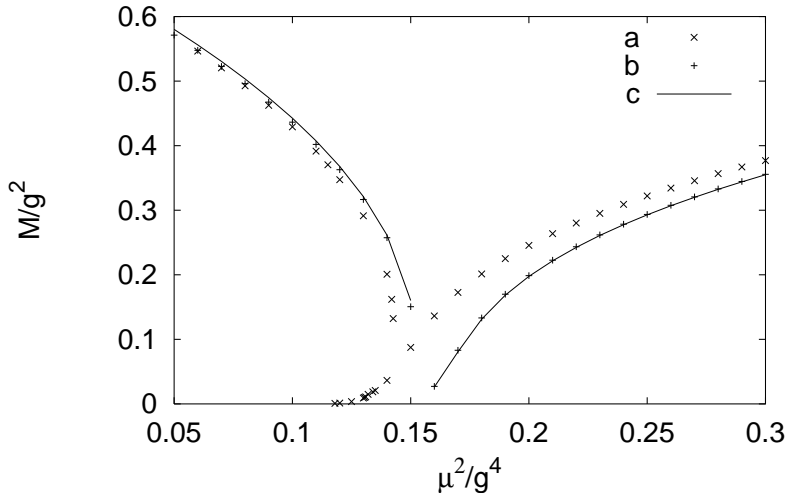


Figure 17: The Higgs boson mass in units of g^2 as function of μ^2/g^4 calculated at $\lambda/g^2 = 1/32$ in the Landau gauge in the full static theory and in the A_0 -reduced theory. Shown are the Higgs mass in the reduced theory obtained by perturbative reduction (a), in the reduced theory obtained by non-perturbative matching (cf. eqs. (109), (110)) (b) and in full static theory (c).

λ/g^2	A		B		C	
	$\xi = 0$	$\xi = 1$	$\xi = 0$	$\xi = 1$	$\xi = 0$	$\xi = 1$
1/32	0.1516	0.1423	0.1426	0.1341	0.1499	0.1405
1/48	0.1647	0.1558	0.1627	0.1541	0.1637	0.1546
1/64	0.1841	0.1750	0.1881	0.1808	0.1875	0.1792

Table. 1: Values of μ_+^2/g^4 in the full static theory (A), in the perturbatively reduced theory (B) and in the reduced theory obtained using non-perturbative matching described in the text (C).

Calculations were done in the Landau ($\xi = 0$) and in the Feynman ($\xi = 1$) gauges.

The endpoint of the 1st order line in the Landau gauge in the 3d Higgs theory was found at $\lambda_c/g^2 = 0.058$. The corresponding critical scalar coupling in the full 3d theory is within the 1% range. In Feynman gauge we find $\lambda_c/g^2 = 0.078$ for the A_0 -reduced theory and the corresponding value for the full 3d theory lies again very close to it. Thus the A_0 field has almost no effect on the position of the endpoint. The strong gauge dependence of λ_c indicates, however, that higher order corrections to this quantity are important.

The gauge dependence of the screening masses is even more pronounced deep in the symmetric phase ($\mu^2/g^4 > 0.3$). For example the value of the gauge boson mass is roughly $0.28g^2$ in the symmetric phase for the Landau gauge. The corresponding value in the Feynman gauge is about $0.22g^2$. The gauge dependence of the gauge boson mass is somewhat weaker at the 2-loop level [80]. It should be also noticed that the gauge boson mass depends weakly on the parameters of the scalar sector (μ , μ_D , λ , λ_A). This fact was also noticed in previous investigations [70, 76].

5.3 Screening Masses in the Symmetric Phase with a Gauge Invariant Resummation Scheme

The main motivation for the present investigation was to gain insight into the decoupling of the dynamics of the fundamental and the adjoint Higgs fields. The degree of the decoupling is expected to depend on the mass ratio of the fundamental and adjoint Higgs fields. In the symmetric phase both masses are of the same order in magnitude (eg. $\sim gT$). Therefore the hierarchy of the A_0 and Higgs masses can only be present due to numerical prefactors. The persistence of the perturbatively calculated ratio should be checked in any non-perturbative approach.

As we have seen in the previous section the gauge dependence in the symmetric phase is too strong in the applied schemes to give a stable estimate for the mass ratio of the fundamental and the adjoint Higgs fields. A reliable non-perturbative estimate for the Higgs mass deep in the symmetric phase (defined through the pole of the propagator) is even more interesting because it was not measured so far on lattice. Therefore, in this section we will investigate a coupled set of gap equations in the symmetric phase which is based on the gauge invariant resummation scheme of Alexanian and Nair (AN) [72]. In this approach one can avoid any vacuum expectation value for the Higgs field in the symmetric phase and because of this fact this approach is gauge invariant.

To derive the gap equations in this scheme one has to add and subtract the mass generating term defined by Eq. (64) and also add the corresponding gauge fixing term defined by Eq. (69). Among diagrams shown in Appendix B those which contain gauge boson propagators should be reevaluated. Straightforward calculations lead to the following equations:

$$\begin{aligned} m_T^2 &= Cg^2m_T + \frac{g^2m_T}{4\pi} \left(2f(m_D/m_T) + f(M/m_T) \right), \\ M^2 &= \mu^2 + \frac{1}{4\pi} \left(\frac{3}{4}g^2MF(M/m_T) - 6\lambda M - 6cm_D \right), \\ m_D^2 &= \mu_D^2 + \frac{1}{4\pi} \left(2g^2m_DF(m_D/m_T) - 5\lambda_A m_D - 8cM \right), \end{aligned} \quad (111)$$

where $C = \frac{1}{4\pi}(21/4 \ln 3 - 1)$ [72] and the following functions were introduced

$$f(z) = -\frac{1}{2}z + \left(z^2 - \frac{1}{4}\right) \operatorname{arctanh} \frac{1}{2z}, \quad (112)$$

$$F(z) = -1 - \frac{1}{z} + \left(4z - \frac{1}{z}\right) \ln(1 + 2z). \quad (113)$$

Let us first discuss the ratio of the A_0 and the fundamental Higgs masses. In Figure 18 this ratio is shown as calculated from the eqs. (111) and compared with the corresponding perturbative value. The μ interval in this plot corresponds to the temperature range relevant for the electroweak theory $T < 1TeV$. We have also analyzed the μ -dependence of the fundamental Higgs mass alone in the full static and in the A_0 -reduced model. For μ^2/g^4 in the interval (0.2 – 0.3) the result of the gauge invariant approach agrees fairly well with the masses obtained in the BP-scheme. In Figure 19 the difference between the Higgs masses calculated from the coupled set of gap equations (111) and the leading order perturbative

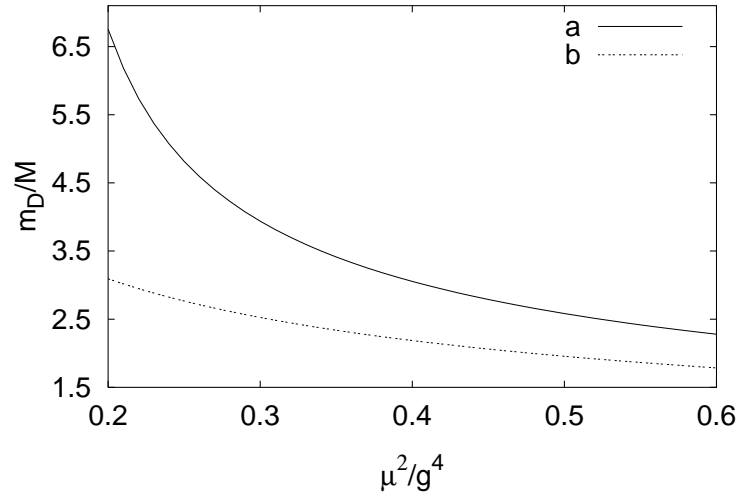


Figure 18: The ratio of the Debye and the fundamental Higgs masses for $\frac{\lambda}{g^2} = 1/8$ calculated from gap eqs. (111) (a) and the leading order result (b).

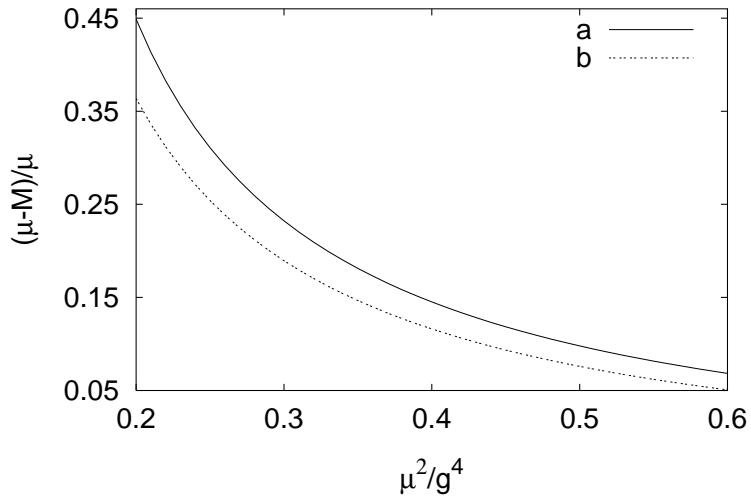


Figure 19: The non-perturbative correction to the Higgs mass as the function of μ calculated from the full static (a) and from the A_0 -reduced theory (b).

result (M_0) is shown. As one can see, the non-perturbative correction to the Higgs mass is the largest for small μ and is decreasing as μ increases reaching the percent level for large enough μ .

The relative difference between the full static and the A_0 -reduced theory, however, is slowly increasing as μ increases and the hierarchy between the A_0 and the Higgs masses becomes less pronounced as μ gets larger. The relative difference between the Higgs masses calculated in the full static and in the A_0 -reduced theory varies between 20% for $\mu^2/g^4 = 0.2$ and 35% for $\mu^2/g^4 = 0.6$.

It is also important to notice that the A_0 field is not sensitive to the dynamics of the Higgs field. In particular it turns out that m_D depends weakly on μ and λ in the symmetric phase and its value is close to the corresponding value calculated in 3d adjoint Higgs model. Let us notice that the magnetic mass in this resummation scheme also seems to be insensitive to the dynamics of scalars, therefore the magnetic and electric screening masses are close to their values determined in the pure SU(2) gauge model.

6 Conclusions

In my Thesis I have studied the problem of screening in hot non-Abelian plasma. A detailed review of the phenomenon of chromoelectric screening was given. It was shown that the chromoelectric screening is a well understood phenomenon in the leading order of perturbation theory and it is quite similar to the well known Debye screening phenomenon in non-relativistic electron plasma. Beyond the leading order, however, it turns out to be very complicated and at present it is even not fully clear how to define it properly. In my numerical investigations Debye screening phenomenon was defined through the long distance (small momentum) behaviour of the static longitudinal propagator. It has been shown that such a definition is free of infrared singularities in higher orders of perturbation theory only if one introduces the so-called magnetic screening mass, a concept which was introduced long ago by Linde to cure infrared divergencies of finite temperature gauge theories [17].

In recent years the problem of magnetic mass was actively studied using self-consistent resummation of perturbative series. The introduction of the magnetic mass allows a self-consistent determination of the Debye screening mass (the inverse screening length) through coupled gap equations, which was discussed in section 3. It was argued that such determination so far is only possible in the framework of the dimensionally reduced effective theory. Thus one has to address the question how far the dimensionally reduced effective theory faithfully represents the high temperature limit of gauge theories. This question is far from being trivial since the separation of different mass scales $2\pi T \gg gT \gg g^2 T$ which is necessary for dimensional reduction is not satisfied for any realistic temperature range in the theory which corresponds to quantum chromodynamics because the gauge coupling constant g is large. This observation suggested that the electric (Debye) and the magnetic screening masses should be determined simultaneously from the coupled set of gap equation. In section 3 where the screening masses were studied through coupled gap equation the precision of dimensional reduction was tested also by examining the effect of non-local operators and it turned out that their contribution is small thus justifying the approach based on dimensional reduction.

In section 4 the screening masses were studied using lattice Monte-Carlo technique in the 3d effective theory corresponding to the high temperature phase of SU(2) gauge theory, the 3d adjoint Higgs model. Comparison of the screening masses obtained in these simulations with the corresponding masses obtained recently in the full 4d finite temperature theory [49] allows to test non-perturbatively and quantitatively the precision of the dimensionally reduced theory. It was shown that the predictions of the 3d effective theory are quite reasonable even at temperature $\sim 4T_c$ and become more and more precise as the temperature is increased. This fact gives prospects for studying the screening phenomena in the effective theory approach. The predictions of the gap equation approach were compared with the corresponding results. It turns out that the results obtained from coupled gap equations describe correctly the temperature dependence of the screening masses, however, so far there is no quantitative agreement between the predictions of the coupled gap equations and the Monte-Carlo data. The Debye mass measured in lattice Monte-Carlo simulations is about 25% larger than what is predicted from the coupled set of gap equations.

In section 5 the screening masses of the finite temperature SU(2) Higgs model were studied. Though the application of the dimensional reduction approach here seems to be more

justified (the corresponding gauge coupling constant is $g \sim 0.66$), the non-perturbative quantitative test of the precision of the dimensional reduction is also important here. The study of the screening masses in this model through coupled gap equations tests the decoupling of the heavy A_0 field (temporal component of the static gauge field). Detailed numerical analysis revealed high precision decoupling of the A_0 field if in the mapping of the full static theory onto the A_0 -reduced system its mass determined non-perturbatively is used. This observation also implies that for the realistic value of the A_0 mass perturbative integration over the heavy A_0 field has limited precision due to the coupling of the heavy A_0 field to the light magnetostatic sector. This coupling to the magnetostatic sector is taken into account in the proposed non-perturbative mapping procedure. It is very interesting that this coupling between the heavy A_0 field and the light magnetostatic sector can be described quite precisely by the magnetic mass obtained from the gap equations.

From the above discussion it is clear that the concept of the magnetic screening mass is extremely useful since it allows higher order definition of the electric screening mass, which quantitatively agrees with the corresponding lattice predictions and also the high quality mapping onto the effective theory mentioned above. The values of magnetic mass determined in different resummation schemes are quite close to each other. A recent 2-loop gap equation of the magnetic mass has shown that the value of the magnetic mass does not change dramatically relative to the 1-loop results and the corresponding value was found to be $0.34g_3^2$ [80] (which should be compared with the 1-loop predictions $0.28g_3^2$ and $0.38g_3^2$). Moreover the non-perturbative analysis of the mass gap in 3d pure gauge theory yields a very similar value $0.32g_3^2$ [81]. All these facts give us confidence that the magnetic mass is a viable concept. However, in Refs. [78, 79] some inconsistencies in the 1-loop determination of the magnetic mass were found. In the numerical simulations the value of the magnetic mass was found to be $\sim 0.46g_3^2$ which is substantially larger than the predictions from the analytical approaches. Thus I think, further studies are required to clarify the phenomenon of non-Abelian magnetic mass generation.

Appendices

A Calculation of Different Diagrams in SU(N) Adjoint Higgs Model

The propagators of different fields can be read off the quadratic part of the Lagrangian. These exact propagators are listed below. The gauge boson propagator:

$$D_{ij}(k) = \left(\delta_{ij} - \frac{k_i k_j}{k^2} \right) \frac{1}{k^2 + m_T^2} + \frac{k_i k_j}{k^2} \frac{\xi}{k^2 + m_L^2}, \quad (\text{A.1})$$

where $m_L = \sqrt{\xi} m_T$, the propagator for the adjoint scalar field A_0 :

$$D^{A_0}(k) = \frac{1}{k^2 + m_D^2}, \quad (\text{A.2})$$

and finally, the ghost propagator:

$$\Sigma(k) = \frac{1}{k^2 + m_G^2}. \quad (\text{A.3})$$

The Feynman diagrams contributing to the 2-point functions of the relevant fields are shown below. In these diagrams every line corresponds to a resummed propagator. The wavy line corresponds to the gauge bosons, the solid one to A_0 and the dashed one to the ghost. The corresponding analytic expressions can be written in terms of the following standard integrals:

$$\begin{aligned} I(k, r, s) &= \int \frac{d^d p}{(2\pi)^d} \frac{1}{(p+k)^{2r} p^{2s}} \\ &= \frac{k^{d-2(r+s)} \Gamma(r+s-\frac{d}{2}) \Gamma(\frac{d}{2}-s) \Gamma(\frac{d}{2}-r)}{(4\pi)^{d/2} \Gamma(r)\Gamma(s) \Gamma(d-s-r)}, \end{aligned} \quad (\text{A.4})$$

$$\begin{aligned} I^m(k, r, s) &= \int \frac{d^d p}{(2\pi)^d} \frac{p_m}{(p+k)^{2r} p^{2s}} \\ &= -k^m \frac{k^{d-2(r+s)} \Gamma(r+s-\frac{d}{2}) \Gamma(\frac{d}{2}+1-s) \Gamma(\frac{d}{2}-r)}{(4\pi)^{d/2} \Gamma(r)\Gamma(s) \Gamma(d+1-s-r)}, \end{aligned} \quad (\text{A.5})$$

$$\begin{aligned} I^{mn}(k, r, s) &= \int \frac{d^d p}{(2\pi)^d} \frac{p^m p^n}{(p+k)^{2r} p^{2s}} \\ &= \frac{k^{d-2(r+s)}}{(4\pi)^{d/2}} \left[\frac{k^2 \Gamma(r+s-1-\frac{d}{2}) \Gamma(\frac{d}{2}+1-s) \Gamma(\frac{d}{2}+1-r)}{2 \Gamma(r)\Gamma(s) \Gamma(d+2-s-r)} \delta^{mn} \right. \\ &\quad \left. + \frac{\Gamma(r+s-\frac{d}{2}) \Gamma(\frac{d}{2}+2-s) \Gamma(\frac{d}{2}-r)}{\Gamma(r)\Gamma(s) \Gamma(d+2-s-r)} k^m k^n \right], \end{aligned} \quad (\text{A.6})$$

$$J(k, m_1, m_2) = \int \frac{d^3 p}{(2\pi)^3} \frac{1}{((p+k)^2 + m_1^2)(p^2 + m_2^2)} = \frac{A}{8\pi}, \quad (\text{A.7})$$

$$J^m(k, m_1, m_2) = \int \frac{d^3 p}{(2\pi)^3} \frac{p_m}{((p+k)^2 + m_1^2)(p^2 + m_2^2)}$$

$$= \frac{k^m}{8\pi} \left[\frac{m_1 - m_2}{k^2} - \frac{k^2 + m_1^2 - m_2^2}{2k^2} A \right], \quad (\text{A.8})$$

$$J^{mn}(k, m_1, m_2) = \int \frac{d^3p}{(2\pi)^3} \frac{p^m p^n}{((p+k)^2 + m_1^2)(p^2 + m_2^2)} \quad (\text{A.9})$$

$$= -\frac{\delta^{mn}}{8\pi} \left[\frac{m_1}{2} + \frac{4k^2 m_2^2 + (k^2 + m_1^2 - m_2^2)^2}{8k^2} A \right] \\ - \frac{k^m k^n}{8\pi} \left[\frac{m_1}{2k^2} - \frac{4k^2 m_2^2 + 3(k^2 + m_1^2 - m_2^2)^2}{8k^4} A \right] \\ + \frac{1}{8\pi} \frac{(m_1 - m_2)(k^2 + m_1^2 - m_2^2)}{4k^2} \left[\delta^{mn} - 3 \frac{k^m k^n}{k^2} \right], \quad (\text{A.10})$$

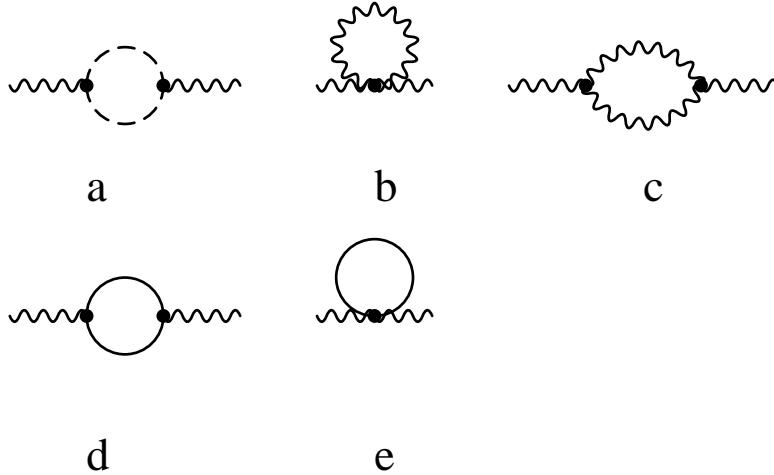
where $A = \frac{2}{k} \arctan\left(\frac{k}{m_1+m_2}\right)$

$$j(m) = \int \frac{d^3p}{(2\pi)^3} \frac{1}{p^2 + m^2} = -\frac{m}{4\pi}, \quad (\text{A.11})$$

$$l^{mn}(m) = \int \frac{d^3p}{(2\pi)^3} \frac{p_m p_n}{p^2 + m^2} = -\frac{\delta^{mn}}{3} m^2 j(m). \quad (\text{A.12})$$

These integrals were evaluated using dimensional regularization.

The diagrams contributing to the 2-point functions of A_i are the following:



with the analytical contribution:

$$\Pi_{ab}^{(a)mn}(k) = g^2 N \delta_{ab} \left[J_{mn}(k, m_G, m_G) + k_m J_n(k, m_G, m_G) \right], \quad (\text{A.13})$$

$$\Pi_{ab}^{(b)mn} = g^2 N \delta_{ab} \delta^{mn} \left[\frac{4}{3} j(m_T) + \frac{2}{3} \xi j(m_L) \right], \quad (\text{A.14})$$

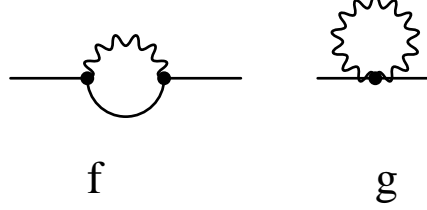
$$\Pi_{ab}^{(c)mn}(k) = -\frac{1}{2} g^2 N \delta_{ab} \left\{ \delta_{mn} \left[-\frac{(m_T^2 + k^2)^2}{m_T^2} (J(k, m_T, 0) + J(k, 0, m_T)) \right. \right. \\ \left. \left. + \frac{2k^2 (4m_T^2 + k^2)}{m_T^2} J(k, m_T, m_T) - 2 \left(1 + \frac{k^2}{m_T^2} \right) j(m_T) \right] \right\}$$

$$\begin{aligned}
& +k_mk_n \left[-\frac{(m_T^2 + k^2)^2}{4m_T^4} J(k, m_T, 0) + \left(\frac{k^4}{4m_T^4} - \frac{k^2}{m_T^2} - 6 \right) J(k, m_T, m_T) \right. \\
& + \left(-\frac{k^4}{4m_T^4} + \frac{3}{2} \frac{k^2}{m_T^2} + \frac{7}{4} \right) J(k, 0, m_T) + \frac{3}{2m_T^2} j(m_T) + \frac{k^4}{4m_T^4} I(k, 1, 1) \Big] \\
& + \left[-\frac{k_mk_n}{m_T^2} j(m_T) + \frac{k^4}{4m_T^4} I_{mn}(k, 1, 1) + \left(\frac{k^4}{4m^4} + 4\frac{k^2}{m_T^2} + 8 \right) J_{mn}(k, m_T, m_T) \right. \\
& - \frac{2}{m_T^2} l_{mn}(m_T) - \left(1 + \frac{k^2}{m_T^2} \right)^2 (J_{mn}(k, 0, m_T) + J_{mn}(k, m_T, 0)) \Big] \\
& + \left[-\frac{k_mk_n}{m_T^2} j(m_T) + \frac{k^4}{m_T^4} k_m I_n(k, 1, 1) - \left(\frac{k^2}{m_T^2} + 1 \right) \left(\frac{k^2}{m_T^2} + 3 \right) k_m J_n(k, m_T, 0) \right. \\
& + \left(1 - \frac{k^4}{m_T^4} \right) k_m J_n(k, 0, m_T) + \left(\frac{k^4}{m_T^4} + 4\frac{k^2}{m_T^2} + 8 \right) k_m J_n(k, m_T, m_T) \Big] \Big\} \\
& -g^2 N \delta_{ab} \xi \left\{ \delta_{mn} \left[\frac{(m_T^2 + k^2)^2}{m_L^2} (J(k, 0, m_T) - J(k, m_L, m_T)) \right. \right. \\
& \quad \left. \left. + \frac{(m_T^2 + m_L^2 + k^2)}{m_L^2} j(m_L) \right] \right. \\
& + \frac{k_mk_n}{4m_T^2 m_L^2} \left[\left(6k^2 m_T^2 + 7m_T^4 + 2m_T^2 m_L^2 - (m_L^2 + k^2)^2 \right) J(k, m_L, m_T) \right. \\
& \quad + m_L^2 j(m_T) - 7m_T^2 j(m_L) + (k^4 - 6k^2 m_T^2 - 7m_T^4) J(k, 0, m_T) \\
& \quad \left. - k^4 I(k, 1, 1) + (m_L^2 + k^2)^2 J(k, m_L, 0) \right] \\
& + \frac{1}{m_L^2 m_T^2} \left[m_T^2 k_m k_n j(m_L) + k^4 (J_{mn}(k, m_L, 0) - I_{mn}(k, 1, 1)) \right. \\
& \quad \left. + (k^2 + m_T^2)^2 (J_{mn}(k, 0, m_T) - J_{mn}(k, m_L, m_T)) + m_T^2 l_{mn}(m_L) \right] \\
& + \left[-\frac{(k^2 + m_T^2)(k^2 - m_T^2 + m_L^2)}{m_L^2 m_T^2} k_m J_n(k, m_L, m_T) - \frac{k^4}{m_L^2 m_T^2} k_m I_n(k, 1, 1) \right. \\
& \quad \left. + \frac{k_mk_n}{m_L^2} j(m_L) + \frac{k^2}{m_T^2} \left(\frac{k^2}{m_L^2} + 1 \right) k_m J_n(k, m_L, 0) + \frac{k^4 - m_T^4}{m_T^2 m_L^2} k_m J_n(k, 0, m_T) \right] \Big\} \\
& -\frac{1}{2} N \delta_{ab} \xi^2 \left\{ \frac{k_mk_n}{4m_L^4} \left[-2m_L^2 j(m_L) + k^4 (I(k, 1, 1) + J(k, m_L, m_L)) \right. \right. \\
& \quad \left. \left. - (k^2 + m_L^2)^2 J(k, m_L, 0) - (k^2 - m_L^2)^2 J(k, 0, m_L) \right] \right. \\
& + \frac{k^4}{m_L^4} \left[I_{mn}(k, 1, 1) - J_{mn}(k, m_L, 0) - J_{mn}(k, 0, m_L) + J_{mn}(k, m_L, m_L) \right] \\
& + \left[-\frac{k^2}{m_L^2} \left(\frac{k^2}{m_L^2} + 1 \right) k_m J_n(k, m_L, 0) - \frac{k^2}{m_L^2} \left(\frac{k^2}{m_L^2} - 1 \right) k_m J_n(k, 0, m_L) \right. \\
& \quad \left. + \frac{k^4}{m_L^4} (k_m J_n(k, m_L, m_L) + k_n I_m(k, 1, 1)) \right] \Big\}, \tag{A.15}
\end{aligned}$$

$$\Pi_{ab}^{(d)mn}(k) = -\frac{1}{2} g^2 N \delta_{ab} \left[4J^{mn}(k, m_D, m_D) + 4k^m J^n(k, m_D, m_D) + k^m k^n J(k, m_D, m_D) \right] \tag{A.16}$$

$$\Pi_{ab}^{(e)mn} = g^2 N \delta_{ab} \delta^{mn} j(m_D). \quad (\text{A.17})$$

Diagrams a), b) and c) were calculated in [19] using the Landau gauge ($\xi = 0$). The results of these calculations coincide with ours if in the above formulas one sets $\xi = 0$. The diagrams contributing to the 2-point function of A_0 are given by diagrams f) and g):

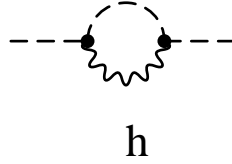


The corresponding analytical contribution is:

$$\begin{aligned} \Pi_{ab}^{(f)\mu\nu}(k) = & -g^2 N \delta_{ab} \delta^{0\mu} \delta^{0\nu} \left[j(m_T) - \frac{k^2 + m_D^2}{m_T^2} j(m_T) - \frac{(m_D^2 + k^2)^2}{m_T^2} J(k, m_D, 0) \right. \\ & \left. + \frac{1}{m_T^2} \left(2k^2 (m_T^2 + m_D^2) + k^4 + (m_T^2 - m_D^2)^2 \right) J(k, m_D, m_T) - j(m_D) \right] \\ & - g^2 N \delta_{ab} \delta^{0\mu} \delta^{0\nu} \frac{\xi}{m_L^2} \left[(m_L^2 + m_D^2 + k^2) j(m_L) + (m_D^2 + k^2)^2 J(k, m_D, 0) \right. \\ & \left. - (m_D^2 + k^2)^2 J(k, m_D, m_L) \right], \end{aligned} \quad (\text{A.18})$$

$$\Pi_{ab}^{(g)\mu\nu} = g^2 N \delta_{ab} \delta^{0\mu} \delta^{0\nu} \left[2j(m_T) + \xi j(m_L) \right]. \quad (\text{A.19})$$

Finally the single diagram contributing to the ghost 2-point function is given by diagram h):



The corresponding analytical contribution is:

$$\begin{aligned} \Sigma_{ab}(k) = & -\frac{1}{2} g^2 N \delta_{ab} \left\{ \left[\frac{m_T^2 - (k^2 + m_G^2)}{4m_T^2} j(m_T) - \frac{(k^2 + m_G^2)^2}{4m_T^2} J(k, m_G, 0) \right. \right. \\ & \left. \left. + \left(\frac{(k^2 + m_G^2)^2}{4m_T^2} + \frac{k^2 - m_G^2}{2} + \frac{m_T^2}{4} \right) J(k, m_G, m_T) - \frac{1}{4} j(m_G) \right] \right. \\ & - \xi \left[\left(\frac{(k^2 + m_G^2)^2}{4m_L^2} + \frac{k^2 + m_G^2}{2} + \frac{m_L^2}{4} \right) J(k, m_G, m_L) - \frac{1}{4} j(m_G) \right. \\ & \left. \left. - \frac{(k^2 + m_G^2)^2}{4m_L^2} J(k, m_G, 0) - \frac{3m_L^2 + k^2 + m_G^2}{4m_L^2} j(m_L) \right] \right\}. \end{aligned} \quad (\text{A.20})$$

B 3d Adjoint Higgs Model on Lattice

B.1 Phase Diagram of 3d Adjoint Higgs Model and Dimensional Reduction

As it was discussed in section 2 the high temperature limit of 4d SU(N) theory is described by 3d adjoint Higgs model with the following action

$$S = \int d^3x \left(\frac{1}{4} F_{ij}^a F_{ij}^a + \frac{1}{2} (D_i A_0^a)^2 + \frac{1}{2} m_{D0}^2 A_0^a A_0^a + \lambda_A (A_0^a A_0^a)^2 \right), \quad (\text{B.21})$$

The relations between the parameters appearing in this equation and those of the original 4d SU(N) theory are [34]

$$g_3^2 = g^2(\mu) T \left[1 + \frac{g^2}{16\pi^2} (L + c_g) \right], \quad (\text{B.22})$$

$$m_{D0}^2 = \frac{1}{3} \left(N + \frac{1}{2} N_f \right) g^2(\mu) T^2 \left[1 + \frac{g^2}{16\pi^2} (L + c_m) \right], \quad (\text{B.23})$$

$$\lambda_A = (6 + N - N_f) \frac{g^4(\mu) T}{24\pi^2} \left[1 + 2 \frac{g^2}{16\pi^2} (L + c_l^{(N)}) \right], \quad (\text{B.24})$$

where

$$L = \frac{22N}{3} \ln \frac{\mu}{\mu_T} - \frac{4N_f}{3} \ln \frac{4\mu}{\mu_T}, \quad (\text{B.25})$$

$$c_g = \frac{N}{3}, \quad (\text{B.26})$$

$$c_m = \frac{10N^2 + 2N_f^2 + 9N_f/N}{6N + 3N_f}, \quad (\text{B.27})$$

$$c_l^{(2)} = \frac{7/3 - 109N_f/96}{1 - N_f/8} + \frac{2}{3} N_f, \quad (\text{B.28})$$

$$c_l^{(3)} = \frac{7/2 - 23N_f/18}{1 - N_f/9} + \frac{2}{3} N_f \quad (\text{B.29})$$

with $\mu_T = 4\pi e^{-\gamma_E} T \sim 7.0555T$. One can easily verify that the parameters g_3^2 , m_{D0} and λ_A do not depend on the renormalization scale μ at leading order. Following Ref. [34] we introduce the following dimensionless parameters which will be useful in further analysis

$$x = \frac{\lambda_A}{g_3^2}, \quad y = \frac{m_{D0}^2}{g_3^4}. \quad (\text{B.30})$$

The lattice action corresponding to the continuum action (B.21) using standard discretization procedure could be written as

$$\begin{aligned} S_A = & \beta \sum_P U_P + \sum_{\mathbf{x}, \hat{i}} 2 \left[\text{Tr} a A_0^2(\mathbf{x}) - \text{Tr} a A_0(\mathbf{x}) U_i(\mathbf{x}) A_0(\mathbf{x} + \hat{i}) U_i^\dagger(\mathbf{x}) \right] \\ & + \sum_{\mathbf{x}} \left[(\tilde{m}_0 a)^2 \text{Tr} a A_0^2(\mathbf{x}) + a \lambda_A (\text{Tr} a A_0^2)^2 \right], \end{aligned} \quad (\text{B.31})$$

where the first term is the standard Wilson action for the gauge fields, $A_0 = \sum_b \tau^b A_0^b$ with τ^b being the generators of the SU(N) gauge group and a is the lattice spacing. Furthermore,

$$\beta = \frac{2N}{g_3^2 a} \quad (\text{B.32})$$

and \tilde{m}_0 is the cutoff dependent bare mass of the A_0 field calculated in lattice regularization. In the following we will consider only the SU(2) case. In order to relate the results of lattice calculations to the physics of the high temperature phase of the original 4d SU(2) gauge theory, it is necessary to find the relation between the bare mass \tilde{m}_0 and the renormalized mass at scale μ in \overline{MS} scheme $m_D^r(\mu)$. Since the theory is superrenormalizable the only running coupling is the mass parameter. The scale dependence of the renormalized mass is given by [34]

$$m_D^r(\mu) = m_{D0} + \frac{5(2g_3^2 - \lambda_A)\lambda_A}{16\pi^2} \ln \frac{g_3^2}{\mu}. \quad (\text{B.33})$$

The bare mass \tilde{m}_0 could be written as

$$\tilde{m}_0 = m_D^r(\mu) + \delta\tilde{m}(\mu), \quad (\text{B.34})$$

where

$$\delta\tilde{m}(\mu) = -\frac{3.1759114}{4\pi a}(4g_3^2 + 5\lambda_A) - \frac{g_3^4}{16\pi^2} \left[(20x - 10x^2)(\ln \frac{6}{a\mu} + 0.09) + 8.7 + 11.6x \right] \quad (\text{B.35})$$

is the 2-loop lattice counterterm calculated in Ref. [102]. It is convenient to write the lattice action in terms of antihermitian matrices \tilde{A}_0 defined by $\beta\tilde{A}_0 = 2ia^{1/2}A_0$. Furthermore introducing the bare mass parameter $h = \tilde{m}_0^2 a^2$ and taking into account that

$$\lambda_A \text{Tr} (aA_0^2)^2 = x\beta \left(\frac{1}{2} \text{Tr} \tilde{A}_0^2 \right)^2 \quad (\text{B.36})$$

the lattice action could be written in the form

$$S = \beta \sum_P \frac{1}{2} \text{Tr} U_P + \beta \sum_{\mathbf{x}, \hat{i}} \frac{1}{2} \text{Tr} \tilde{A}_0(\mathbf{x}) U_i(\mathbf{x}) \tilde{A}_0(\mathbf{x} + \hat{i}) U_i^\dagger(\mathbf{x}) + \sum_{\mathbf{x}} \left[-\beta \left(3 + \frac{1}{2}h \right) \frac{1}{2} \text{Tr} \tilde{A}_0^2(\mathbf{x}) + \beta x \left(\frac{1}{2} \text{Tr} \tilde{A}_0^2(\mathbf{x}) \right)^2 \right]. \quad (\text{B.37})$$

Making use of Eqs. (B.34) and (B.35) the bare mass parameter h could be written in terms of β and continuum parameters x and y as

$$h(x) = \frac{16}{\beta^2} y - \frac{3.1759114(4 + 5x)}{\pi\beta} - \frac{1}{\pi^2\beta^2} \left((20x - 10x^2)(\ln \frac{3}{2}\beta + 0.09) + 8.7 + 11.6x \right). \quad (\text{B.38})$$

The phase diagram of the 3d SU(2) adjoint Higgs model was established in Ref. [34] in terms of x and y using multicanonical update technique [103]. It has a symmetric (confinement) phase and the broken (Higgs) phase separated for small x by a line of 1st order phase transition. The transition becomes weaker as x increases and eventually turns to a crossover

for some $x > 0.3$. However, dimensional reduction is applicable only for temperatures larger than the critical which means that physically relevant values of x are smaller than 0.2. The transition line was obtained by fitting different data points with a polynomial and was found to be (see Figure 20)

$$xy_c = 2/(9\pi^2)(1 + 9/8x + Ax^{3/2} + Bx^2 + Cx^{5/2} + Dx^3), \quad (\text{B.39})$$

where $A = 45.1(2.9)$, $B = -214.7(20.2)$, $C = 350.7(44.5)$, $D = -206.7(31.4)$.

The physics of the high temperature SU(2) gauge theory corresponds to some line in xy -plane, the *line of 4d physics* $y_{4d}(x)$. This line can be calculated using Eqs.(B.22)-(B.24) and for SU(2) it has the following form

$$y_{4d}(x) = \frac{(8 - N_f)(4 + N_f)}{144\pi^2 x} + \frac{192 - 2N_f - 7N_f^2 - 2N_f^3}{96(8 - N_f)\pi^2}. \quad (\text{B.40})$$

The position of $y_{4d}(x)$ relative to $y_c(x)$ determines the physical phase of the 3d adjoint Higgs model. It turns out the for physically interesting values of x $y_{4d}(x) < y_c(x)$ and the physical phase is the broken one. The corresponding situation is shown in Figure 20.

The fact that the broken phase corresponds to the high temperature phase is self-contradictory because dimensional reduction is valid if $A_0 \ll \sqrt{T}$, but in the broken phase $A_0 \sim 1/g$. However, the line of 4d physics lies in the region where the symmetric phase is still metastable for finite lattice volume as it is indicated in Figure 20. Using this fact it was suggested in Ref. [34] that one can perform simulations along the line of 4d physics $y_{4d}(x)$ analyze samples in the symmetric branch of the mixed phase. The obvious problem with this approach is that the metastable phase disappears in the infinite volume limit.

A different approach for fixing parameters appearing in Eq. (B.37) was proposed in Ref. [26]. This approach is based on matching different quantities calculated with weak coupling expansion in the 4d lattice gauge theory and the corresponding 3d effective theory at some small physical distance, where the weak coupling expansion is applicable. In this approach the bare mass parameter is given by [26]

$$h = g^2 \left(\tilde{\Pi}_{00} + 2L_0^{-1} \left[2 \frac{1}{L_s^3} \sum_{\mathbf{k} \neq 0} \frac{1}{4 \sum_{i=1}^3 \sin^2(k_i/2)} + \frac{1}{12L_s^3} \right] \right), \quad (\text{B.41})$$

where L_0 and L_s are the temporal and spatial lattice sizes of the original 4d lattice and g is the 4d gauge coupling. $\tilde{\Pi}_{00}$ was calculated in Ref. [104]. The other two couplings appearing in the lattice action are given by

$$\beta = \frac{4}{L_0 g^2 (1 + \alpha g^2)} \quad (\text{B.42})$$

$$x = \frac{g^2}{(3\pi^2(1 + \alpha g^2))}, \quad (\text{B.43})$$

where α is a slightly volume dependent factor. The gauge coupling g was found by matching the Polyakov loop correlator measured in Monte-Carlo simulations to its perturbative

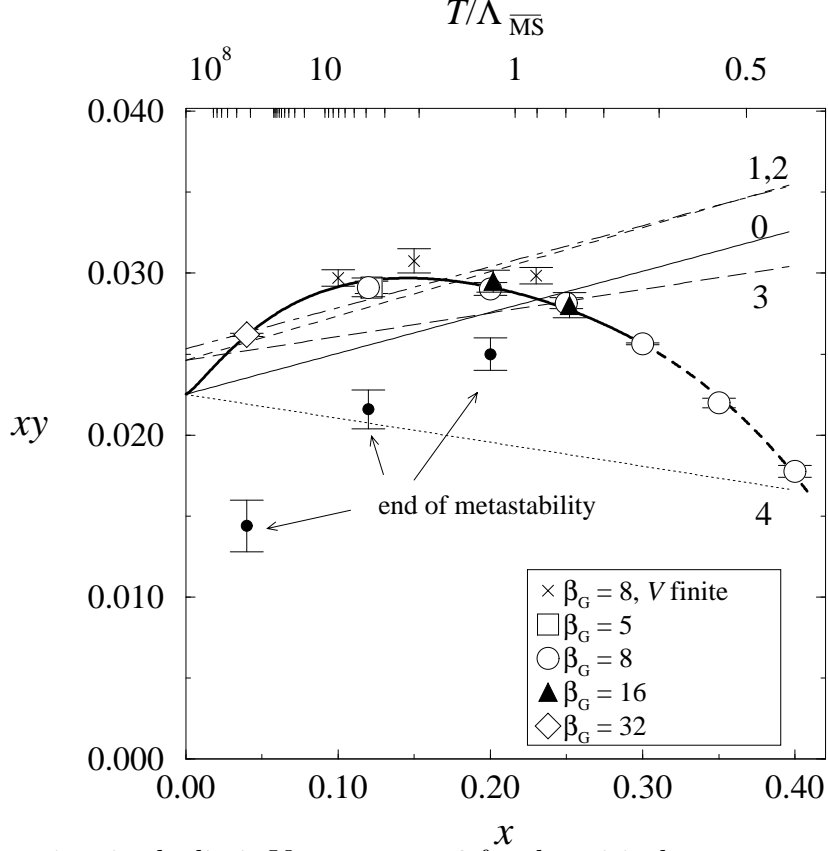


Figure 20: Data points in the limit $V \rightarrow \infty, a \rightarrow 0$ for the critical curve $y = y_c(x)$ (multiplied by x). The thick line is the fit to the $V = \infty$ extrapolated data. The dashed line marks the region where the transition turns into a cross-over. The straight lines are the 4d \rightarrow 3d curves of eq. (B.40) marked by the value of N_f . The top scale shows the values of $T/\Lambda_{\overline{\text{MS}}}$ (Figure is taken from Ref. [34]).

expression at distance $R = (4T)^{-1}$ [104]. The numerical values of the coupling for lattices considered in Ref. [26] together with the physical temperature are summarized in the following Table ¹⁷

	T/T_c	g^2	β	h	x
4×16^3 ($\alpha = -0.06$) ($\tilde{\Pi}_{00} = -0.0384$)	3.5	1.26	13.70	-0.28	0.046
	6.0	1.18	14.60	-0.27	0.043
4×24^3 ($\alpha = -0.059$) ($\tilde{\Pi}_{00} = -0.0431$)	2.0	1.43	12.25	-0.31	0.053
	3.5	1.28	13.54	-0.28	0.047
	6.0	1.19	14.48	-0.26	0.043

Table 5: Parameters of the effective theories for different temperatures and lattice volumes according Ref.[26].

¹⁷The numerical values of h given in [26] are not correct. The correct values of h calculated from Eq. (B.41) are slightly different from those given in Ref.[26].

Now we look for the physical phase in this approach. This question was addressed in Ref. [28] and it was concluded that the physical space is the symmetric one. In Ref. [28] the values of h corresponding to the phase transition were determined for 4×12^3 , 4×16^3 and 4×24^3 lattices and found to be $h_c = -0.2623(1)$, $-0.2803(1)$ and $-0.30(1)$. Extrapolation to infinite volume yields $-0.2943(2)$. Now using Eq. (B.38) we can evaluate h_c from the result of the polynomial fit for $y_c(x)$ given by Eq. (B.39) at $x \sim 0.047$ and $\beta = 13.54$, which yields $h_c = -0.2733(25)$. Thus the values of h corresponding to the transition are underestimated. We can estimate the infinite volume limit of h defined by Eq. (B.41), the calculation yields $h = -0.2699$. However, Eq. (B.41) is only valid at 1-loop level, at 2-loop level h is given by Eq. (B.38) which yields -0.2789 which definitely corresponds to the broken phase. Therefore the conclusion that the symmetric phase is the physical reached in [28] is sensitive to the approximation made in the analysis, and thus is unreliable.

B.2 Extracting the Screening Masses from the Propagators

For the analysis of the large distance behaviour of the propagators it is convenient to introduce the so-called local masses. They are defined by the following relation

$$\frac{G_i(z)}{G_i(z+1)} = \frac{\cosh(m_i(z)(z - N_z/2))}{\cosh(m_i(z)(z + 1 - N_z/2))}, \quad (\text{B.44})$$

where $i = D, T$ and the corresponding propagators are defined by Eqs. (79) and (80) and N_z is the extension of the lattice in z direction. If the propagators show exponential decay starting from some value of z the corresponding local masses reach a plateau. Therefore the local masses are useful in defining the starting point of the fit interval. In order to determine properly the fit interval correlated fit should be used together with the χ^2 criteria. If one uses simple uncorrelated fit the corresponding values of $\chi^2/d.o.f$ are very small which does not allow to choose the fit interval properly. In Figure 21 the local magnetic masses measured on $16^2 \times 64$ lattice at $\beta = 8$, $x = 0.09$ and $y = 0.4007$ are shown. The filled squares denotes the data points which were used in the fit and yields good $\chi^2/d.o.f$. The fit based on this data points yields the value $0.422(6)g_3^2$ for the magnetic mass. In Ref. [93] the magnetic mass was measured in the symmetric phase of the 3d SU(2) Higgs model. The magnetic mass for the 3d pure gauge theory was also determined there and its value was found to be somewhat larger but close to the corresponding value of the 3d Higgs model. In Ref. [93] the magnetic masses were extracted from propagators using uncorrelated fit over the interval $[8, N_z - 8]$ with the following fit ansatz

$$G_T(z) = A \left(\exp(-m_T z) + \exp(-m_T(N_z - z)) \right) + B \quad (\text{B.45})$$

where the propagators were measured for $\beta = 9$ on $16^2 \times N_z$ lattice, with $N_z = 32 - 128$. For $N_z = 64$ the value of the magnetic mass was found to be $0.39(2)g_3^2$ (see Table 1 in Ref. [93]). Using the same procedure for our data we obtain $m_T = 0.408(8)g_3^2$ which is compatible with the result of Ref.[93]. However, most of simulations in Ref. [93] were done on $16^2 \times 32$ lattice. On this lattice the magnetic mass was found to be $0.35(1)g_3^2$.

In order to get in contact with the results of Ref.[93] we have performed simulations on $16^2 \times 32$ lattice at $\beta = 9$ in 3d pure gauge theory and extracted the magnetic mass using

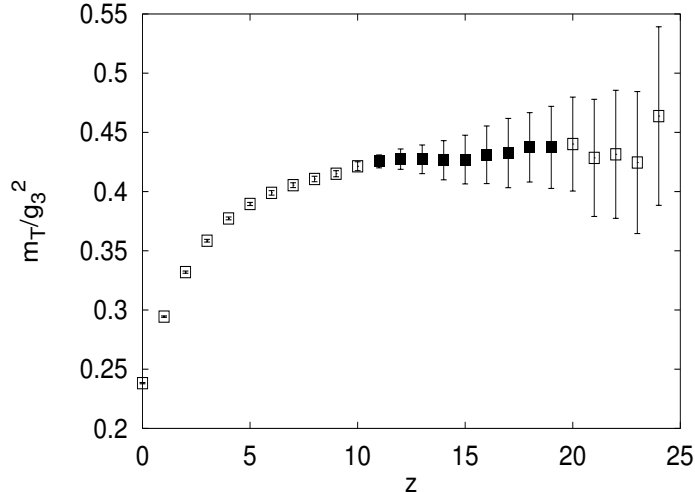


Figure 21: The local magnetic masses in units of g_3^2 as function of z measured at $\beta = 8$, $x = 0.09$ and $y = 0.4007$. The filled squares denote the data points used for extracting the magnetic screening mass

the procedure outlined above. The corresponding value of the magnetic mass was found to be $0.39(3)g_3^2$. This value is smaller than corresponding value obtained by us for $16^2 \times 64$ lattice and this is probably due to the fact that on such lattices the magnetic mass cannot be reliably determined because the local masses do not show a plateau (see Figure 2 in Ref. [93]). We think that the small difference between this value and the corresponding value found in Ref.[93] is probably due to the presence of the Higgs fields.

The above analysis shows the importance of the finite size effects and the proper procedure of extracting the screening masses.

B.3 The Dependence of the Screening Masses on the Choice of the Temperature Scale and Lattice Spacing

As it was already explained in section 4.1 the temperature scale in the effective theory is set by parameter x and its relation to the renormalized 4d gauge coupling $g(T)$. In section 4.1 $g(T)$ was determined by the 2-loop formula in \overline{MS} scheme with $\mu = 2\pi T$. It seems to be interesting to examine to what extent the numerical results on the screening masses presented in section 4.3 depend on the definition of $g(T)$ and/or the choice of the renormalization scale. In Figure 22 the temperature dependence of the screening masses is shown for the case when the temperature scale is set by the 1-loop level renormalized coupling

$$g^{-2}(T) = \frac{11}{12\pi^2} \ln \frac{\mu}{\Lambda_{\overline{MS}}} \quad (\text{B.46})$$

with $\mu = 2\pi T$ and $\Lambda_{\overline{MS}} = T_c/1.06$. As one can see from Figure 22 the screening masses are systematically overestimated compared to the 4d results in this case.

It was mentioned in section 4.4 that the square root of the spatial string tension in the deconfined phase of the 4d SU(2) gauge theory is expected to scale with $g_3^2 \sim g(T)^2 T$. This

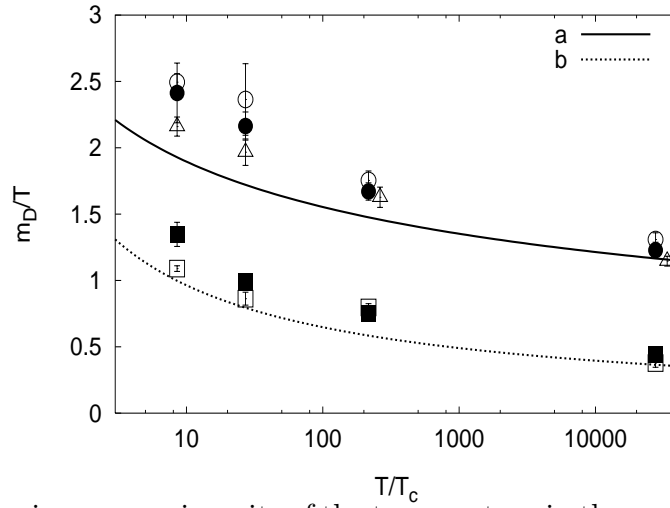


Figure 22: The screening masses in units of the temperature in the case when the temperature scale is set by the 1-loop level renormalized coupling (see text for details) Shown are the Debye mass m_D for the first (filled circles) and the second (open circles) set of h , and the magnetic mass m_T for the first (filled squares) and the second (open squares) set of h . Also shown there are the values of the Debye mass measured in metastable phase along the perturbative line of 4d physics (open triangles). The line (a) and line (b) represent the fit for the temperature dependence of the Debye and the magnetic mass from 4d simulations from [49]. Some data points at the temperature $T \sim 260T_c$ and $\sim 30000T_c$ have been shifted in the temperature scale for better visualization.

fact can be used for non-perturbative definition of $g(T)$. In Ref. [91] it was found that the temperature dependence of the square root of the spatial string tension is well described by the formula

$$\sqrt{\sigma_s(T)} = (0.369 \pm 0.014)g^2(T)T \quad (\text{B.47})$$

if the running coupling constant g is chosen according to

$$g^{-2}(T) = \frac{11}{12\pi^2} \ln \frac{T}{\Lambda_T} + \frac{17}{44\pi^2} \ln \left[2 \ln \frac{T}{\Lambda_T} \right]. \quad (\text{B.48})$$

with $\Lambda_T = 0.076(13)T_c$ [91]. This running coupling constant $g(T)$ is equivalent to the 2-loop running coupling in \overline{MS} scheme if the renormalization scale is chosen to be $\mu \sim 13.3T$. However the data on the temperature dependence of the spatial string tension can be also well fitted with the formula $\sqrt{\sigma_s(T)} = (0.334 \pm 0.014)g^2(T)T$ if $g(T)$ is chosen according to

$$g^{-2}(T) = \frac{11}{12\pi^2} \ln \frac{T}{\Lambda_T} \quad (\text{B.49})$$

with $\Lambda_T = 0.050(10)T_c$ [91]. This running coupling corresponds to the running coupling constant in \overline{MS} scheme with $\mu \sim 20T$. The value of the string tension in 3d SU(2) gauge theory is $\sqrt{\sigma_3} = 0.3340(25)g_3^2$ [92]. Now if the temperature scale is set by the running coupling $g(T)$ defined by Eq. (B.46) but with $\mu \sim 20T$ very good agreement between the 3d and 4d data is found.

From the above analysis it is clear that the definitions of $g(T)$ and values of the normalization scale μ which yield good agreement between 3d and 4d data are compatible with values of g found non-perturbatively from the analysis of the spatial string tension. On the other hand the values of gauge coupling used in Ref. [26] are by factor of 2 smaller than these.

The matching analysis in section 4.3 was done at $\beta = 16$. It is important to check the sensitivity of these results to the choice of β which defines the lattice spacing. The dependence of the Debye masses on β was analyzed for $x = 0.05$ and for all three values of y (h) used in our matching analysis. The corresponding results are shown in Table 6.

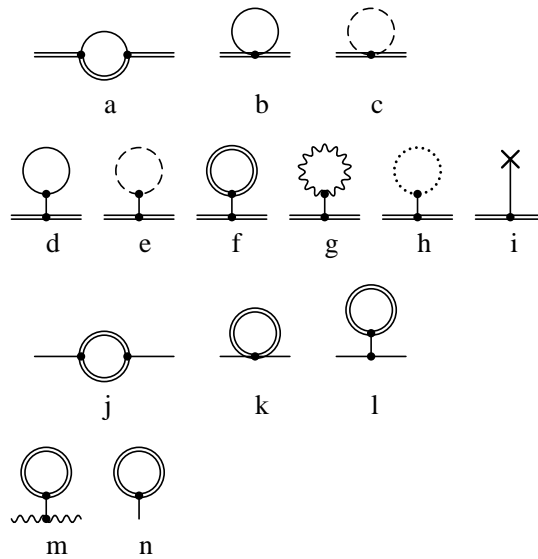
β	12	16	20
$y = 0.6721$	1.84(21)	1.69(6)	1.68(12)
$y = 0.5914$	1.57(6)	1.68(4)	1.65(6)
$y = 0.4756$	—	1.48(5)	1.44(12)

Table 6: Debye masses for different values of β for $x = 0.05$

As one can see from the results presented in Table 6 no lattice spacing dependence for the Debye mass can be observed. A similar analysis should be done for the magnetic mass. But for $\beta = 20$ the magnetic mass can be measured reliably only for lattices larger than 32×64 . Using the fact that the magnetic mass calculated in the 3d adjoint Higgs model is close to the magnetic mass of 3d pure gauge theory one and based on results presented in section 4.4 we can conclude that the magnetic mass also does not depend on β .

C Self-energy Contributions in 3d fundamental + adjoint Higgs model

Below we list graphically the additional diagrams contributing to the A_0 (**a-i**), Higgs boson (**j-l**) and the vector boson (**m**) self-energies and the vacuum expectation value (**n**). Here solid lines denotes the propagator of the Higgs field, dashed lines corresponds to Goldstone fields, double line corresponds to the adjoint Higgs field and finally the dotted line corresponds to ghost fields. Wavy lines as usually corresponds to vector fields.



References

- [1] J.I. Kapusta, Finite Temperature Field Theory (Cambridge University Press, 1989)
- [2] M. Le Bellac, Thermal Field Theory (Cambridge University Press, 1996)
- [3] A. Dolgov, Phys. Rep. **222** (1992) 311
- [4] V.A. Rubakov and M. E. Shaposhnikov, Usp. Fiz. Nauk **166** (1996) 493 [hep-ph/9603208]
- [5] J. Kuti, J. Polónyi and K. Szlachányi, Phys. Lett, **B98** (1981)
- [6] L.D. McLerran and B. Svetitsky, Phys. Rev. **D24** (1981) 450
- [7] X.-N. Wang, Phys. Rep. **280** (1997) 287
- [8] H. Satz, Talk given at International Conference on the Physics and Astrophysics of the Quark-Gluon Plasma, Jaipur, India, March 15-21, 1997
- [9] E. Braaten and R.D. Pisarski, Nucl. Phys. **B337** (1990) 569; *ibid.* **B339** (1990) 310; Phys. Rev. Lett. **64** (1990) 2242; Phys. Rev. **D42** (1990) 2156
- [10] A. Jakovác, K. Kajantie and A. Patkós, Phys. Rev. **D49** (1994) 6891
- [11] K. Farakos, K. Kajantie, K. Rummukainen and M. Shaposhnikov, Nucl. Phys. **B425** (1994) 67
- [12] K. Kajantie, M. Laine, K. Rummukainen and M. Shaposhnikov, Nucl. Phys. **B458** (1996) 90
- [13] E. Braaten, Phys. Rev. Lett. **74** (1995) 2164
- [14] E. Braaten and A. Nieto, Phys.Rev. **D53** (1996) 3421; Phys. Rev. Lett. **76** (1996) 1417
- [15] P. Lévai and U. Heinz, Phys. Rev. **C57** (1998) 1879 (and references therein)
- [16] P. Lévai and R. Vogt, Phys. Rev. **C56** (1997) 2707
- [17] A.D. Linde, Phys. Lett. **B96** (1980) 289
- [18] W. Buchmüller and O. Philipsen, Phys. Lett, **B397** (1997) 112
- [19] K. Kajantie, M. Laine, K. Rummukainen and M. Shaposhnikov, Nucl. Phys. **B466** (1996) 189
- [20] K. Kajantie, M. Laine, K. Rummukainen and M. Shaposhnikov, Phys. Rev. Lett. **77** (1996) 2887
- [21] K. Kajantie, M. Laine, K. Rummukainen and M. Shaposhnikov, Nucl. Phys. **B493** (1997) 413

- [22] P. Ginsparg, Nucl. Phys. **B170** (1980) 388
- [23] T. Appelquits and R. Pisarski, Phys. rev. **D23** (1981) 6990
- [24] N. P. Landsman, Nucl. Phys. **B322** (1989) 498
- [25] T. Reisz, Z. Phys. **53** (1992) 169
- [26] P. Lackock, D.E. Miller and T. Reisz, Nucl. Phys. **B369** (1992) 501
- [27] L. Kärkkäinen, P. Lackock, D.E. Miller, B. Petersson and T. Reisz, Phys. Lett. **B282** (1992) 121; L. Kärkkäinen, P. Lackock, B. Petersson and T. Reisz, Nucl. Phys. **B395** (1993) 733
- [28] L. Kärkkäinen, P. Lackock, D.E. Miller, B. Petersson and T. Reisz, Nucl. Phys. **B418** (1994) 3
- [29] P. Arnold and L. G. Yaffe, Phys. Rev. **D52** (1995) 7208
- [30] K. Kajantie, M. Laine, J. Peisa, A. Rajantie, K. Rummukainen and M. Shaposhnikov, Phys. Rev. Lett. **79** (1997) 3130;
- [31] M. Laine and O. Philipsen, Nucl. Phys. **B523** (1998) 267
- [32] M. Laine and O. Philipsen, hep-lat/9905004
- [33] S. Bronoff, R. Buffa, C. P. Korthals Altes, hep-ph/9801333
- [34] K. Kajantie, M. Laine, K. Rummukainen and M. Shaposhnikov, Nucl. Phys. **B503** (1997) 357
- [35] J.-P. Blaizot and E. Iancu, Nucl. Phys. **417** (1994) 608
- [36] P.F. Kelly, Q. Liu, C. Lucchesi and C. Manuel, Phys. Rev. Lett. **72** (1994) 3461; Phys. Rev. **D50** (1994) 4209
- [37] S. Wong, Nuovo Cimento **65A** (1970) 689
- [38] F. Karsch, M. Lütgemeier, A. Patkós and J. Rank, Phys. Lett. **B390** (1996) 291
- [39] T. Appelquist and J. Carrazzone, Phys. Rev. **D11** (1975) 2856
- [40] A. Jakovác and A. Patkós, Nucl. Phys. **B494** (1997) 291
- [41] T. Toimela, Z. Phys. **C27** (1985) 289
- [42] R. Kobes, G. Kunstatter and A. Rebhan, Phys. Rev. Lett. **64** (1990) 2992; Nucl. Phys. **B355** (1991) 1
- [43] A. Rebhan, Nucl. Phys. **B430** (1994) 319
- [44] L. Dolan and R. Jackiw, Phys. Rev. **D9** (1974) 3320

- [45] A. Billoire, G. Lazarides and Q. Shafi, Phys. Lett. **B103** (1980) 450
- [46] T.A. DeGrand and D. Toussaint, Phys. Rev. **D25** (1982) 526
- [47] T.S. Bíró and B. Müller, Nucl. Phys. **A561** (1993) 477
- [48] U.M. Heller, F. Karsch and J. Rank, Phys. Lett. **B355** (1995) 511
- [49] U.M. Heller, F. Karsch and J. Rank, Phys. Rev. **D57** (1998) 1438
- [50] F. Karsch, M. Oevers and P. Petreczky, Phys. Lett. **B442** (1998) 291
- [51] S. Nadkarni, Phys. Rev. **D22** (1986) 3738
- [52] E. Braaten and A. Nieto, Phys. Rev. Lett. **74** (1995) 3530
- [53] E. Shuryak, JETP, **47** (1978) 212
- [54] J. Kapusta, Nucl. Phys. **B148**, (1979) 461
- [55] K. Kalashnikov and J. Klimov, Sov. J. Nucl. Phys. **33** (1981) 647
- [56] A. Toimela, Phys. Lett. **B124** (1983) 407
- [57] P. Arnold and C. Zhai, Phys. Rev. **D50** (1994) 7603 and Phys. Rev. **D51** (1995) 1906
- [58] B. Kastening and C. Zhai, Phys. Rev. **D52** (1995) 7232
- [59] A. Nieto, Int. J. Mod. Phys. **A12** (1997) 1431
- [60] F. Karsch, A. Patkós and P. Petreczky, Phys. Lett. **B401** (1997) 69
- [61] J. Reinbach and H. Schulz, Phys. Lett. **B404** (1997) 291
- [62] I.T. Drummond, R.R. Horgan, P.V. Landshoff and A. Rebhan, Nucl. Phys. **B524** (1998) 579
- [63] J. Frenkel, A. Saa, and J. Taylor, Phys. Rev. **D46** (1992) 3670
- [64] R. Parwani, Phys. Rev. **D45** (1992) 4965
- [65] D.J. Amit, Field Theory, Renormalisation Group and Critical Phenomena, chapter 7, p.173
- [66] F. Karsch, A. Patkós and P. Petreczky, Screened Perturbation Theory, Proceedings of the Workshop on Strong and Electroweak Matter'97, 21-25 May 1997, Eger, Hungary, Eds. F. Csikor and Z. Fodor, p.424
- [67] J.R. Espinosa, M. Quirós and F. Zwirner, Phys. Lett. **B314** (1993) 206
- [68] W. Buchmüller, Z. Fodor, T. Helbig and D. Walliser, Ann. Phys. **234** (1994) 260
- [69] J.O. Andersen, E. Braaten and M. Strickland, hep-ph/9902327; hep-ph/9905337

- [70] W. Buchmüller and O. Philipsen, Nucl. Phys. **B443** (1995) 47
- [71] O. Philipsen, On the problem of the Magnetic Mass, Proceedings of the NATO Advanced Research Workshop on Electroweak Physics and the Early Universe, Sintra, Portugal, 23-25 March 1994, Eds. J.C. Romão and F. Freire, p. 393
- [72] G. Alexanian and V. P. Nair, Phys. Lett. **352** (1995) 435
- [73] R. Jackiw and S.-Y. Pi, Phys. Lett. **B403** (1997) 297
- [74] P. Arnold and O. Espinosa, Phys. Rev. **D47** (1993) 3546
- [75] A. Jakovác, Phys. Rev. **D53** (1996) 4538
- [76] A. Patkós, P. Petreczky, Zs. Szép, Eur. Phys. J **C5** (1998) 337
- [77] A. Jakovác and A. Patkós, Phys. Lett. **B334** (1994) 391
- [78] R. Jackiw, Phys. Lett. **B368** (1996) 131
- [79] J. Cornwall, Phys. Rev. **D57** (1998) 3694
- [80] F. Eberlein, Phys. Lett. **B439** (1998) 130; Nucl. Phys. **B550** (1999) 303
- [81] V.P. Nair, Talk given at 5th Workshop on Thermal Field Theories and their Applications, August 1998, Regensburg, Germany, hep-th/9809086 (and references therein)
- [82] S. Nadkarni, Nucl. Phys. **B334** (1990) 559
- [83] A. Hart, O. Philipsen, J.D. Stack and M. Tepper, Phys. Lett. **B396** (1997) 217
- [84] J. Polónyi and S. Vazquez, Phys. Lett. **B240** (1990) 183
- [85] S. Bronoff, PhD Thesis (unpublished)
- [86] J.E. Mandula and M. Ogilvie, Phys. Lett. **B185** (1987) 127
- [87] J.E. Mandula and M. Ogilvie, Phys. Lett. **B248** (1990) 156
- [88] C. Bernard, A. Soni and K. Yee, Nucl. Phys. (Proc. Suppl.) **20** (1991) 410
- [89] W. Dimm, P. Lepage and P.B. Mackenzie, Nucl. Phys. (Proc. Suppl.) **42** (1995) 403
- [90] C. Michael and A. McKerrel, Phys. Rev. **D51** (1995) 3745
- [91] G.S. Bali, J. Finberg, U.M. Heller, F. Karsch and K. Schilling, Phys. Rev. Lett. **71** (1993) 3059
- [92] M. Teper, Phys. Lett. **B289** (1992) 115
- [93] F. Karsch, T. Neuhaus, A. Patkós and J. Rank, Nucl. Phys. **B474** (1996) 189

- [94] O. Philipsen, Talk given at Workshop on Strong and Electroweak Matter'98, Copenhagen, 2-5 December, 1998, to be published in the Proceedings of the workshop [hep-ph/9902376]
- [95] A.S. Kronfeld, Phys. Rev. **D58** (1998) 051501.
- [96] F. Karsch, M. Oevers and P. Petreczky, Talk given at Workshop on Strong and Electroweak Matter'98, Copenhagen, 2-5 December 1998, to be published in the Proceedings of the workshop [hep-ph/9902373]
- [97] Y. Aoki, F. Csikor, Z. Fodor, A. Ukawa, hep-lat/9901021
- [98] F. Csikor, Z. Fodor, J. Heitger, Phys. Rev. Lett. **82** (1999) 21
- [99] M. Laine, hep-ph/9903513
- [100] P. Petreczky, Zs. Szép and A. Patkós, hep-ph/9905269
- [101] A. Rebhan, Next-to-Leading Order Debye-Screening in Spontaneously Broken Gauge Theories, Proceedings of the NATO Advanced Research Workshop on Electroweak Physics and the Early Universe, Sintra, Portugal, 23-25 March 1994, Eds. J.C. Romão and F. Freire, p. 397 [hep-ph/9404292]
- [102] M. Laine, Nucl. Phys. **B451** (1995) 484
- [103] B. Berg and T. Neuhaus, Phys. Lett. **B267** (1991) 249
- [104] A. Irbäck, P. Lacock, D.E. Miller, B. Petersson and T. Reisz, Nucl. Phys. **B363** (1991) 34

Acknowledgements

A substantial part of the work presented in this thesis was carried out at the University of Bielefeld under the supervision of Prof. Karsch. Numerical Monte-Carlo simulations have been performed on CRAY T3E at HLRZ Jülich and at High Performance Computing Center Stuttgart. I thank the Peregrination II Fund and Center of Interdisciplinary Research (ZiF) for the financial support during my stay at the University of Bielefeld. Travel grants from the doctoral program of Eötvös University are gratefully acknowledged. I am grateful to Prof. Patkós for giving many useful advice during the preparation of this thesis. Different parts of the work presented in this thesis profited much from enjoyable discussions with W. Buchmüller, Z. Fodor, A. Jakovác, O. Philipsen and K. Rummukainen. I am also grateful to O. Philipsen and K. Rummukainen for sending some of their numerical data and e-mail correspondence. I thank M. Oevers and Zs. Szép for collaboration. Finally I thank my parents and my wife for their support during my graduate studies.